Published OnlineFirst December 3, 2010; DOI:10.1158/1078-0432.CCR-10-1287

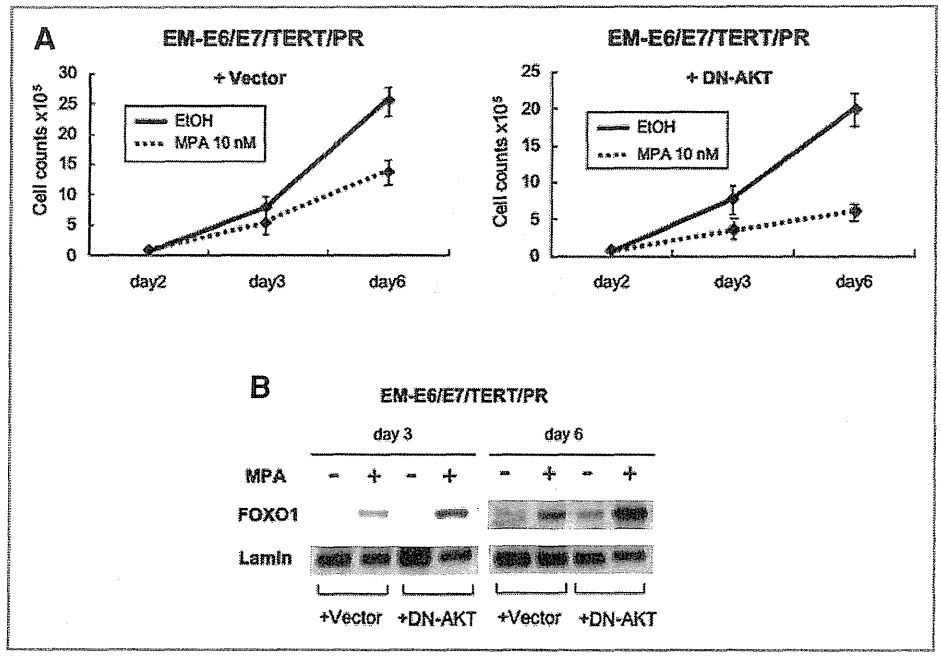

Figure 7. Akt activity limits the MPA effect. A, EM-E6/E7/TERT/PR/DN-AKT or EM-E6/E7/TERT/PR/vector cells were established from EM-E6/E7/TERT/PR cells by retroviral transfection of dominant negative *Akt* gene or blank vector, respectively. These cells were treated with or without MPA for different periods, and the cell number was counted to evaluate the proliferative activity. Data are presented as mean ± SD of the three independent experiments. B, western blot analysis was performed using nuclear extracts of EM-E6/E7/TERT/PR/DN-AKT or EM-E6/E7/TERT/PR/vector cells in the absence or presence of MPA on day 3 or day 6 to compare the levels of nuclear FOXO1 induction. Data are presented as mean ± SD of the three independent experiments.

interaction may account for the nuclear accumulation. Further mechanistic study will be needed to clearly dissect molecular mechanisms of nuclear accumulation of FOXO1 by progestin in endometrial epithelial cells.

A role for FOXO1 in inhibiting cell growth has recently been reported using endometrial cancer cell lines *in vitro* (27). Overexpression of a gain-of-function mutant of the FOXO family inhibited the growth of Ishikawa cells that constitutively express low levels of FOXO1, while siRNA inhibition of the *FOXO* gene in HEC-1® cells that express high levels of FOXO1 enhanced their growth. Furthermore, Ward and colleagues also demonstrated that progestins increased FOXO1 protein levels in endometrial cancer cell lines, specifically through PRB (28), supporting our data. A growth inhibitory effect of FOXO family members has been proposed in other cell types, in particular, in vascular cells (29, 30). More recently, a role of the FOXO family as a tumor suppressor has been proposed (31). To circumvent embryonic lethality, Paik and colleagues used an inducible Cre-lox system to knock out the FOXO family: the widespread somatic deletion of these genes caused thymic lymphomas and hemangiomas, which were associated with increased cell proliferation and survival in these lineages (31). What are the downstream targets of FOXO for inhibiting cell growth? Recently, sprouty (Spry2), a negative regulator of receptor tyrosine kinases, was validated as a direct FOXO target to inhibit cell cycle progression and induce apoptosis (31). Several other forkhead-responsive genes have been reported, including Insulin-like growth factor-binding protein-1 (*IGBP-1*), glucose-6-phosphatase, FasL, Trail, and Bim (20, 25, 32–35). However, in DNA microarray and RT-PCR analyses, we failed to observe upregulation of these candidate genes upon MPA stimulation (data not shown). Therefore, at present, it remains unclear how cell cycle arrest at G0/G1 is conferred by FOXO1 in endometrial epithelial cells.

In clinical practice of cancer treatment, we have no reliable parameter to predict the efficacy of MPA therapy. We found that the Akt signal, an upstream inhibitory factor of FOXO family, limits the effect of progestin. As we cannot predict the activation of FOXO by MPA before the treatment, the status of Akt activation could be an alternative predictor of MPA therapy. Our preliminary data show that patients responsive to MPA therapy have decreased p-AKT expression confirmed by immunohistochemistry in pretreated samples. It is well known that RAS signalings lead to AKT activation in various cancers via cross-talk signalings (36). It is therefore possible that activated RAS signalings (such as via *RAS* mutation) disturb MPA responsiveness and is an additional predictor of MPA therapy. In the present study, EM-E6/E7/TERT/RAS/PR cells with oncogenic *KRAS* mutation well responded to MPA (Figs. 2 and 3). These cells exhibit only weak levels of p-AKT expression, lacking AKT activation even with *KRAS* mutation (data not shown). Furthermore, in clinical samples, *KRAS* mutation is not always associated with AKT activation in endometrial cancer (37). Therefore, the status of *RAS* does not appear to be a strong predictor of MPA response, but this point requires further investigation.

In summary, our *in vitro* and *in vivo* treatment model has, for the first time, revealed that progestin targets FOXO via transcriptional activation to inhibit the growth of both non-transformed and transformed endometrial

Published OnlineFirst December 3, 2010; DOI:10.1158/1078-0432.CCR-10-1287

epithelial cells without p21/WAF-1 induction. Further investigations of the FOXO1 target genes as well as of AKT signaling as a predictor of MPA efficacy are required to fully understand the molecular mechanisms of progestin effects and help define patient selection for progestin therapy.

Disclosure of Potential Conflicts of Interest

No potential conflicts of interest were disclosed.

Acknowledgments

We greatly thank Ms. Tamami Ryu for her technical assistance. This study was supported by a grant-in-aid for scientific research from the Japan Society for the Promotion of Science (JSPS) and the Megumi Medical Foundation of Kanazawa University.

The costs of publication of this article were defrayed in part by the payment of page charges. This article must therefore be hereby marked *advertisement* in accordance with 18 U.S.C. Section 1734 solely to indicate this fact.

Received May 14, 2010; revised August 3, 2010; accepted August 5, 2010; published OnlineFirst December 3, 2010.

References

1. Parkin DM, Bray F, Ferlay J, Pisani P. Global cancer statistics, 2002. CA Cancer J Clin 2005;55:74–108.
2. Moore TD, Phillips PH, Nerenstone SR, Cheson BD. Systemic treatment of advanced and recurrent endometrial carcinoma: current status and future directions. J Clin Oncol 1991;9:1071.
3. Creasman WT, Odicino F, Maisonneuve P, Beller U, Benedet JL, Heintz AP, et al. Carcinoma of the corpus uteri. J Epidemiol Biostat 2001;6:47–86.
4. Kaku T, Yoshikawa H, Tsuda H, Sakamoto A, Fukunaga M, Kuwabara Y, et al. Conservative therapy for adenocarcinoma and atypical endometrial hyperplasia of the endometrium in young women: central pathologic review and treatment outcome. Cancer Lett 2001; 167: 39–48.
5. Ushijima K, Yahata H, Yoshikawa H, Konishi I, Yasugi T, Saito T, et al. Multicenter phase II study of fertility-sparing treatment with medroxyprogesterone acetate for endometrial carcinoma and atypical hyperplasia in young women. J Clin Oncol 2007;25:2798–803.
6. Owen GI, Richer JK, Tung L, Takimoto G, Horwitz KB. Progesterone regulates transcription of the p21(WAF1) cyclin-dependent kinase inhibitor gene through Sp1 and CBP/p300. J Biol Chem 1998;273: 10696–701.
7. Migliaccio A, Piccolo D, Castoria G, Di Domenico M, Bilancio A, Lombardi M, et al. Activation of the Src/p21ras/Erk pathway by progesterone receptor via cross-talk with estrogen receptor. EMBO J 1998;17:2008–18.
8. Niemann TH, Yilmaz AG, McGaughy VR, Vaccarello L. Retinoblastoma protein expression in endometrial hyperplasia and carcinoma. Gynecol Oncol 1997;65:232–6.
9. Semczuk A, Miturski R, Skomra D, Jakowicki JA. Expression of the cell-cycle regulatory proteins (pRb, cyclin D1, p16INK4A and cdk4) in human endometrial cancer: correlation with clinicopathological features. Arch Gynecol Obstet 2004;269:104–10.
10. Enomoto T, Fujita M, Inoue M, Rice JM, Nakajima R, Tanizawa O, et al. Alterations of the p53 tumor suppressor gene and its association with activation of the c-K-ras-2 protooncogene in premalignant and malignant lesions of the human uterine endometrium. Cancer Res 1993; 53:1883–8.
11. Kyo S, Nakamura M, Kiyono T, Maida Y, Kanaya T, Tanaka M, et al. Successful immortalization of endometrial glandular cells with normal structural and functional characteristics. Am J Pathol 2003;163:2259–69.
12. Mizumoto Y, Kyo S, Ohno S, Hashimoto M, Nakamura M, Maida Y, et al. Creation of tumorigenic human endometrial epithelial cells with intact chromosomes by introducing defined genetic elements. Oncogene 2006;25:5673–82.
13. Akahira J, Inoue T, Suzuki T, Ito K, Konno R, Sato S, et al. Progesterone receptor isoforms A and B in human epithelial ovarian carcinoma: immunohistochemical and RT-PCR studies. Br J Cancer 2000;81: 1488–94.
14. Akahira J, Inoue T, Suzuki T, Ito K, Konno R, Sato S, et al. Telomerase activation by hTRT in human normal fibroblasts and hepatocellular carcinomas. Nat Genet 1998;18:65–8.
15. Shimizu Y, Takeuchi T, Mizuguchi K, Kiyono T, Inoue M and Kyo S. Dienogest, a synthetic progestin, inhibits the proliferation of immortalized human endometrial epithelial cells with suppression of cyclin D1 gene expression. Mol Hum Reprod 2009;15:693–701.
16. Schreiber E, Matthias P, Muller MM, Schaffner W. Rapid detection of octamer binding proteins with "mini-extracts," prepared from a small number of cells. Nucleic Acids Res 1989;17:6419.
17. Labied S, Kajihara T, Madureira PA, Fusi L, Jones MC, Higham JM, et al. Progestins regulate the expression and activity of the forkhead transcription factor FOXO1 in differentiating human endometrium. Mol Endocrinol 2006;20:35–44.
18. Accili D, Arden KC. FoxOs at the crossroads of cellular metabolism, differentiation, and transformation. Cell 2004;117:421–6.
19. Anderson MJ, Viars CS, Czekay S, Cavenee WK, Arden KC. Cloning and characterization of three human forkhead genes that comprise an FKHR-like gene subfamily. Genomics 1998;47:187–99.
20. Brunet A, Bonni A, Zigmond MJ, Lin MZ, Juo P, Hu LS, et al. Akt promotes cell survival by phosphorylating and inhibiting a forkhead transcription factor. Cell 1999;96:857–68.
21. Buzzio OL, Lu Z, Miller CD, Unterman TG, Kim JJ. FOXO1A differentially regulates genes of decidualization. Endocrinology 2006;147: 3870–6.
22. Grinius L, Kessler C, Schroeder J, Handwerger S. Forkhead transcription factor FOXO1A is critical for induction of human decidualization. J Endocrinol 2006;189:179–87.
23. Lin K, Dorman JB, Rodan A, Kenyon C. daf-16: an HNF-3/forkhead family member that can function to double the life-span of *Caenorhabditis elegans*. Science 1997;278:1319–22.
24. Kops GJ, de Ruiter ND, De Vries-Smits AM, Powell DR, Bos JL, Burgering BM. Direct control of the forkhead transcription factor AFX by protein kinase B. Nature 1999;398:630–34.
25. Dijkers PF, Medema RH, Lammers JW, Loenderman L, Coffer PJ. Expression of the pro-apoptotic Bcl-2 family member Bim is regulated by the forkhead transcription factor FKHR-L1. Curr Biol 2000;10: 1201–04.
26. Takano M, Lu Z, Goto T, Fusi L, Higham J, Francis J, et al. Transcriptional cross talk between the forkhead transcription factor forkhead box O1A and the progesterone receptor coordinates cell cycle regulation and differentiation in human endometrial stromal cells. Mol Endocrinol 2007;21:2334–49.
27. Goto T, Takano M, Albergaria A, Briese J, Pomeranz KM, Cloke B, et al. Mechanism and functional consequences of loss of FOXO1 expression in endometrioid endometrial cancer cells. Oncogene 2008;27:9–19.
28. Ward EC, Hoekstra AV, Blok LJ. The regulation and function of the forkhead transcription factor, forkhead box O1, is dependent on the progesterone receptor in endometrial carcinoma. Endocrinology 2008;149:1942–50.
29. Potente M, Urbich C, Sasaki K, Hofmann WK, Heeschen C, Aicher A, et al. Involvement of Foxo transcription factors in angiogenesis and postnatal neovascularization. J Clin Invest 2005;115:2382–92.

Published OnlineFirst December 3, 2010; DOI:10.1158/1078-0432.CCR-10-1287

30. Abid MR, Yano K, Guo S, Patel VI, Shrikhande G, Spokes KC, et al. Forkhead transcription factors inhibit vascular smooth muscle cell proliferation and neointimal hyperplasia. J Biol Chem 2005;280: 29864–73.
31. Paik JH, Kollipara R, Chu G, Ji H, Xiao Y, Ding Z, et al. FoxOs are lineage-restricted redundant tumor suppressors and regulate endothelial cell homeostasis. Cell 2007;128:309–23.
32. Tomizawa M, Kumar A, Perrot V, Nakae J, Accili D, Rechler MM. Insulin inhibits the activation of transcription by a C-terminal fragment of the forkhead transcription factor FKHR. A mechanism for insulin inhibition of insulin-like growth factor-binding protein-1 transcription. J Biol Chem 2000;275:7289–95.
33. Schmoll D, Walker KS, Alessi DR, Grempler R, Burchell A, Guo S, et al. Regulation of glucose-6-phosphatase gene expression by protein kinase B alpha and the forkhead transcription factor FKHR. Evidence for insulin response unit-dependent and -independent effects of insulin on promoter activity. J Biol Chem 2000;275: 36324–33.
34. Modur V, Nagarajan R, Evers BM, Milbrandt J. FOXO proteins regulate tumor necrosis factor-related apoptosis inducing ligand expression. Implications for PTEN mutation in prostate cancer. J Biol Chem 2002;277:47928–37.
35. Stahl M, Dijkers PF, Kops GJ, Lens SM, Coffer PJ, Burgering BM, et al. The forkhead transcription factor FoxO regulates transcription of p27Kip1 and Bim in response to IL-2. J Immunol 2002;168:5024–31.
36. Cully M, You H, Levine AJ, Mak TW. Beyond PTEN mutations: the PI3K pathway as an integrator of multiple inputs during tumorigenesis. Nat Rev Cancer 2006;6:184–92.
37. Mori N, Kyo S, Sakaguchi J, Mizumoto Y, Ohno S, Maida Y, et al. Concomitant activation of AKT with ERK1/2 occurs independently of PTEN or PIK3CA mutations in endometrial cancer and may be associated with favorable prognosis. Cancer Sci 2007;98:1881–8.

DOI:10.1158/1078-0432.CCR-10-2291

Clinical Cancer Research

Activation of NF-κB Is a Novel Target of *KRAS*-Induced Endometrial Carcinogenesis

Yasunari Mizumoto, Satoru Kyo, Tohru Kiyono, et al.

Clin Cancer Res 2011;17:1341-1350. Published online March 15, 2011.

DOI:10.1158/1078-0432.CCR-10-2291

Human Cancer Biology

Clinical Cancer Research

Activation of NF-κB Is a Novel Target of *KRAS*-Induced Endometrial Carcinogenesis

Yasunari Mizumoto[1], Satoru Kyo[1], Tohru Kiyono[2], Masahiro Takakura[1], Mitsuhiro Nakamura[1], Yoshiko Maida[1], Noriko Mori[1], Yukiko Bono[1], Hiroaki Sakurai[3], and Masaki Inoue[1]

Abstract

Purpose: Although the *KRAS* mutation is one of critical genetic alterations in endometrial carcinogenesis, the downstream targets are not known.

Experimental Design: In this study, we investigated the molecular targets of *KRAS* signals, using tumorigenic cells with oncogenic *KRAS* mutation established from telomerase reverse transcriptase (*TERT*)-immortalized endometrial epithelial cells.

Results: We first confirmed that the RAF-ERK pathway, but not the PI3K-Akt pathway, was activated in *KRAS* tumorigenic cells. However, the introduction of constitutively active MAP/ERK kinase into immortalized cells to mimic RAF-ERK activation failed to obtain tumorigenic phenotypes, indicating the existence of other carcinogenic pathways triggered by *KRAS*. Recent evidence suggestive of linkage with *KRAS* signals prompted us to examine the involvement of NF-κB in endometrial carcinogenesis. We found that the DNA-binding activity of NF-κB was markedly elevated in *KRAS* tumorigenic cells compared with *TERT*-immortalized cells. Furthermore, the ability of NF-κB to activate the target gene promoters significantly increased in *KRAS* tumorigenic cells. Introduction of a mutant IκB that is resistant to degradation and thereby enhances the inhibitory effect on NF-κB largely abrogated the transformed phenotypes of *KRAS* tumorigenic cells. Thus, oncogenic *KRAS* signals contributed to the tumorigenic phenotypes of endometrial cells by activating the transcription function of NF-κB.

Conclusions: These findings clearly show that NF-κB activation is a novel target of oncogenic *KRAS* in endometrial carcinogenesis, implying the potential utility of NF-κB inhibitors for endometrial cancer chemoprevention, especially with *KRAS* mutation. *Clin Cancer Res; 17(6); 1341–50. ©2011 AACR.*

Introduction

The genetic alterations frequently observed in endometrial cancer involve microsatellite instability and mutations in *PTEN*, *PIK3CA*, *β-catenin*, and *KRAS*, whereas a relatively small percentage of endometrial cancers have *p53* mutations (1, 2). Because some of these gene mutations, including *KRAS* mutation, were detected in precursor lesions, they are thought to be early events in endometrial carcinogenesis (1–4). Ras signals activate various effector pathways in a species- or tissue-specific manner (5). However, the Ras downstream signals essential for endometrial carcinogenesis remain unclear.

Authors' Affiliations: [1]Department of Obstetrics and Gynecology, Kanazawa University Graduate School of Medical Science, Kanazawa, Ishikawa; [2]Virology Division, National Cancer Center Research Institute; and [3]Department of Pathogenic Biochemistry, Institute of Natural Medicine, University of Toyama, Toyama, Japan

Corresponding Author: Satoru Kyo, Kanazawa University Graduate School of Medical Science, 13-1 Takaramachi, Kanazawa, Ishikawa 920-8641, Japan. Phone: 81-(0)-76-265-2425; Fax: 81-(0)-76-234-4266; E-mail: satoruky@med.kanazawa-u.ac.jp

doi: 10.1158/1078-0432.CCR-10-2291

The study of human tumor specimens has provided much of our current understanding of the molecular basis of carcinogenesis. However, most human cancers harbor complex karyotypes and multiple genetic mutations, so the specific types and mechanisms of genetic alterations contributing to carcinogenesis remain unclear. One potential way to overcome these issues is to develop a carcinogenesis model, using defined genetic elements. We have previously created an *in vitro* model of endometrial carcinogenesis in which purified endometrial epithelial cells were immortalized by stably introducing HPV16 *E6* and *E7* and the catalytic subunit of telomerase (*hTERT*; resulting in EM-E6/E7/TERT cells; ref. 6), followed by the additive introduction of oncogenic *KRAS* alleles to obtain tumorigenic cells with anchorage-independent growth and tumorigenicity on nude mice (EM-E6/E7/TERT/RAS cells; ref. 7). One of the most important characteristics of the EM-E6/E7/TERT/RAS cells is their genetic purity with intact chromosomes. Therefore, these immortalized and tumorigenic endometrial epithelial cell lines created with defined genetic rearrangements are advantageous and available for analyzing the oncogenic pathways of endometrial carcinogenesis.

NF-κB has been studied extensively as an inducible transcriptional regulator of the immune and inflammatory

DOI:10.1158/1078-0432.CCR-10-2291

Translational Relevance

The signal transduction or oncogenic pathways in endometrial carcinogenesis remain unclear, although some genetic factors, including *PTEN* and *KRAS* mutations and microsatellite instability, have been identified to play etiologic roles in the development of this tumor type. Most researchers believed that KRAS-ERK1/2 pathway plays central roles in it, but few studies have directly proved it. In this study, we for the first time found that the conventional KRAS-ERK1/2 pathway is insufficient for endometrial carcinogenesis and that NF-κB is a critical target of KRAS-induced endometrial carcinogenesis. This information implies the novel molecular mechanisms of endometrial carcinogenesis and the future therapeutic direction for cancer prevention by suppressing this novel pathway, such as with NF-κB inhibitors.

responses. Accumulating evidence supports a key role of the constitutive activation of NF-κB in controlling the initiation and progression of human cancer (8). NF-κB has also been documented both to be activated downstream of oncogenic Ras signals in some types of human cancers and to participate in the transformation of rodent cells (9–11). However, the role of NF-κB in endometrial carcinogenesis remains unclear. In this study, we show for the first time that NF-κB activation plays a central role in *KRAS*-mediated endometrial carcinogenesis.

Materials and Methods

Electrophoretic mobility shift assay

The nuclear extracts were prepared as previously described (12). A consensus oligonucleotide containing the NF-κB binding site (Promega) was end labeled with the kit (MEGALABEL; Takara Bio Inc.). For the assay, 50 μg of nuclear protein extract was incubated for 30 minutes at room temperature in a final volume of 25 μL containing 10,000 cpm of labeled oligonucleotides, 1 μg of poly (dI-dC), 0.5 mmol/L of phenylmethylsulfonylfluoride, 1 mmol/L of dithiothreitol, 10% glycerol, 25 mmol/L of HEPES (pH 7.9), and 50 mmol/L of KCl. DNA–protein complexes were then separated from free probes by electrophoresis on a 5% polyacrylamide gel. For competition assays, 100-fold molar excess of unlabeled consensus oligonucleotides for AP2, SP1, or NF-κB were used as competitors. For supershift assays, the nuclear extracts were incubated with specific antibodies against NF-κB for 30 minutes before addition of the labeled oligonucleotides. Antibodies against p65 (sc-109X) and p50 (sc-114X) were purchased from Santa Cruz Biotechnology, Inc.

Luciferase reporter assay

Cells were cultured in 24-well culture plates and transfected with 0.4 μg of luciferase reporter plasmid driven by NF-κB–responsive elements (Panomics, Inc.), using Lipofectamine Plus (Invitrogen Corp.), according to the manufacturer's protocol. After 48 hours of incubation, the cells were harvested in passive lysis buffer (Promega) and luciferase assays were carried out. To examine the role of IKK (IκB kinase complex) pathways in promoter activation, 5 μmol/L of IKK inhibitor X (Calbiochem) was added to the medium after the reporter transfection. All experiments were carried out at least 3 times, and the results represent average relative luciferase activity.

Establishment of stable transfectants

The plasmid encoding a constitutively active mutant of *MEK1* (HA-MEK1DD; ref. 13) was kindly provided by Dr. S. Meloche (Université de Montréal, Quebec, Canada). HA-MEK1DD and the mutant IκBα cDNA-encoding superrepressor (IκBα-SR) harboring S32A and S36A mutations (Clontech; catalogue no. 6319233) were cloned and recombined into retroviral vectors to generate pCMSCVpuro-HA-MEK1DD and pCMSCVbsd-IκBα (Ser32/36Ala) as described previously (14). The production and infection of recombinant retroviruses have been described previously (6). These retroviruses and backbone vectors were infected into EM-E6/E7/TERT/RAS cells. The infected cells were selected in the presence of 1 mg/mL of puromycin and 8 mg/mL of blasticidin S.

Immunoblot and immunoprecipitation

Whole-cell extracts were prepared as previously described (12), with specific antibodies against phospho-p44/42MAPK (Thr202/Tyr204), Akt, phospho-Akt (Ser473), phospho-NF-κB p65 (Ser536), phospho-NF-κB p65 (Ser276), IκBα (Cell Signaling Technology), IκBε (Abcam), IκBβ (Delta Biolabs), NF-κB p65 phospho-Ser529 (Millipore), NF-κB p52, NF-κB p50, and actin (Santa Cruz Biotechnology). The LAS3000 CCD-Imaging System (Fujifilm Co. Ltd.) was used for the detection and quantification of proteins visualized by ECL Plus Western blotting detection reagents (GE Healthcare UK Ltd.).

Immunoprecipitation was done using Dynabeads Protein G kit (Invitrogen) with antibodies against p65 (sc-8008; Santa Cruz Biotechnology) or normal mouse IgG (sc-2025; Santa Cruz Biotechnology), according to the manufacturer's protocol. Immunoprecipitated lysates were subjected to the Western blot analysis with antibodies against p65 (sc109; Santa Cruz Biotechnology) or IκB (Cell Signaling Technology).

Cell culture and *in vitro* growth assay

Establishment of immortalized (EM-E6/E7/TERT) and tumorigenic (EM-E6/E7/TERT/RAS) endometrial epithelial cells has been described elsewhere (6, 7). Cells were maintained in Dulbecco's modified Eagle's medium (DMEM) supplemented with 10% FBS and penicillin–streptomycin in an atmosphere of 5% CO_2 at 37°C. Growth activity of EM-E6/E7/TERT/RAS cells with overexpressed mutant IκBα (IκBαM) or with control vectors was evaluated in normal serum (10% FBS) or low serum (0.5% FBS) conditions by

DOI:10.1158/1078-0432.CCR-10-2291

counting cell number on days 3, 4, 5, and 6 after the seeding of 5×10^4 cells in 6-cm dishes.

Anchorage independence of growth

A total of 1×10^4 cells was seeded in 60-mm dishes containing a top layer of 0.33% noble agar in DMEM supplemented with 10% FBS and a bottom layer of 0.5% base agar in DMEM supplemented with 10% FBS as described elsewhere (7). The number of colonies larger than 0.05 mm in size after 4 weeks of incubation was counted under a microscope.

Nude mouse xenograft experiments

Cells were resuspended in growth media (10^7 cells/mL) and injected (0.1 mL) subcutaneously at the base of the trunk of female BALB/c *nu/nu* mice (age range, 7–9 weeks; Japan SCL). Tumor size, if any, was monitored weekly for 8 weeks.

Matrigel invasion assay

The invasive ability of cells was assayed *in vitro* using a BioCoat Matrigel Invasion Chamber (Becton Dickinson Biosciences), as described elsewhere (15). Cells were suspended in the upper wells of Matrigel chambers at 2.5×10^4 cells/chamber in DMEM containing 0.1% bovine serum albumin. Chambers were set into 24-well plates with DMEM containing 10% FBS. After 22 hours of incubation, cells on the upper surface of the membrane were removed by wiping with cotton swabs and cells that had migrated through the membrane containing Matrigel to the lower surface were fixed with methanol and stained with Mayer's hematoxylin. The cells on the lower surface of the membrane were counted microscopically as the invasion index. Chemotaxis assays were conducted in the same manner as for chemoinvasion, except that the filters were not coated with Matrigel, and the number of cells on the lower surface of the membrane was counted as the migration index. The invasive ability of cells was described as the relative value of invasion index versus migration index.

Statistical analysis

The data from the anchorage-independent growth assay and Matrigel invasion assay were presented as the mean ±SD of triplicate assays per group. Differences between groups were evaluated using Student's *t* test. The value of $P < 0.05$ was considered to be statistically significant.

Results

RAF-ERK and PI3K-Akt pathways do not play major roles in *KRAS*-induced endometrial carcinogenesis

Numerous effector pathways have been shown downstream of oncogenic *KRAS* signals, including the RAF-ERK and PI3K-Akt pathways. Activation of ERK upregulates the transcription of genes associated with cell proliferation, whereas the activation of Akt leads to the induction of antiapoptotic genes; thus, both ERK and Akt play crucial roles in cancer initiation. We first examined whether either or both pathways were activated by oncogenic *KRAS* signals during endometrial carcinogenesis. As shown in Figure 1, the expression of phosphorylated ERK apparently increased in tumorigenic EM-E6/E7/TERT/RAS cells compared with immortalized control EM-E6/E7/TERT cells whereas phosphorylated Akt expression was not detected in both cell types, suggesting that the RAF-ERK pathway, but not the PI3K-Akt pathway, was activated by oncogenic *KRAS* signals in endometrial cancer cells.

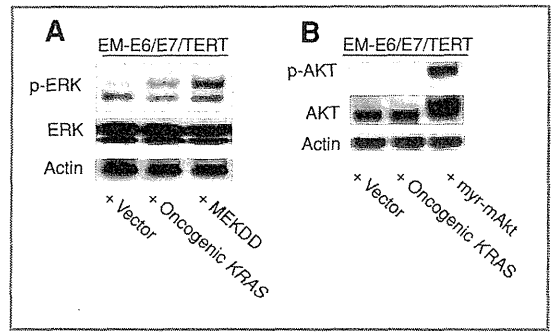

Figure 1. The RAF-ERK pathway, but not the PI3K-Akt pathway, is activated in endometrial epithelial cells transformed by oncogenic *KRAS*. Immortalized endometrial epithelial (EM-E6/E7/TERT) cells were stably transfected with oncogenic *KRAS*, constitutively activated *MEK* (MEKDD), or constitutively activated *Akt* (myr-mAkt) alleles and the expressions of phosphorylated ERK (A) and phosphorylated Akt (B) were examined by Western blot analysis. Cells with constitutively activated *Akt* alleles were used for the positive control of the activated PI3K-Akt pathway.

We next examined the biological roles of RAF-ERK activation in *KRAS*-induced endometrial carcinogenesis. To clarify the role of RAF-ERK signaling, a constitutively active form of the *MEK1* (MEK1 S218D/S222D) allele (16) was retrovirally introduced into EM-E6/E7/TERT cells; these cells were confirmed to express stable and strong levels of p-ERK comparable with those of EM-E6/E7/TERT/RAS cells (Fig. 1A). Then, the phenotypic changes were observed. However, these cells completely lacked anchorage-independent growth or tumorigenicity in mice (Table 1). Thus, ERK activation is not a critical factor to induce transformed phenotypes on oncogenic *KRAS* signals in endometrial epithelial cells.

Table 1. Change in transformed phenotypes of endometrial epithelial cell lines by introducing defined genetic elements

EM-E6/E7/TERT cells	Anchorage-independent growth	Tumorigenicity (BALBc *nu/nu*)
+ Vector	No	No
+ Oncogenic *KRAS*	Yes (100%)	Yes (100%)
+ Active MEK	No	No

DOI:10.1158/1078-0432.CCR-10-2291

Oncogenic *KRAS* enhances the transcriptional function of NF-κB in endometrial cancer cells

On the basis of these results, we sought other candidate factors involved in *KRAS*-induced endometrial carcinogenesis. One such factor is NF-κB, based on emerging evidence that NF-κB is one of the putative effectors of Ras-mediated cellular transformation in rodent cells (9–11). Therefore, we investigated whether the introduction of oncogenic *KRAS* regulates NF-κB activity in EM-E6/E7/TERT cells. First, we examined the change in the DNA-binding activity of NF-κB by electrophoretic mobility shift assay (EMSA), using consensus oligonucleotides for NF-κB and nuclear extracts prepared from EM-E6/E7/TERT/RAS cells or the vector control EM-E6/E7/TERT/vec cells. As shown in Figure 2A, binding complexes were clearly observed in extracts of EM-E6/E7/TERT/vec cells. These bands were apparently intensified in extracts of EM-E6/E7/TERT/RAS cells. However, these bands were completely inhibited in competition assays by the addition of excess amounts of NF-κB consensus oligonucleotides but not by unrelated SP1 or AP2 oligonucleotides. Furthermore, they were supershifted by the addition of antibodies against NF-κB p50 or p65 subunits (Fig. 2B). We confirmed that endogenous expression levels of NF-κB were equivalent in EM-E6/E7/TERT/vec and EM-E6/E7/TERT/RAS cells. These findings indicate that oncogenic *KRAS* facilitates the DNA binding of NF-κB to its target sequences in endometrial cancer cells.

Next, we examined the change in the ability of NF-κB to transactivate the target promoters by oncogenic *KRAS*. Both EM-E6/E7/TERT/KRAS and EM-E6/E7/TERT/vec cells were transfected with the luciferase reporter plasmid containing the NF-κB–responsive elements (pNFκB-luc), and the relative luciferase activities of cell lysates were measured 48 hours after transfection. As shown in Figure 2C, the luciferase activity significantly increased (up to 5-fold) in EM-E6/E7/TERT/RAS cells compared with EM-E6/E7/TERT/vec cells, showing that oncogenic *KRAS* enhances the ability of NF-κB to transactivate the target gene promoter in endometrial cancer cells. Interestingly, this upregulation of NF-κB transcriptional activity was not cancelled by the addition of the MAP/ERK kinase (MEK)-inhibitor U0126, indicating that the RAF-ERK pathway is not involved in this activation. Taken together, we concluded that oncogenic *KRAS* functionally activates NF-κB in endometrial epithelial cells in a RAF-ERK pathway–independent manner.

Inhibition of NF-κB activity abrogates the transformed phenotypes of endometrial cancer cells

Regulation of NF-κB activity is controlled mainly by the inhibitory function of the IκB family, including IκBα. Phosphoryation of IκBα at 2 serine residues (Ser32 and

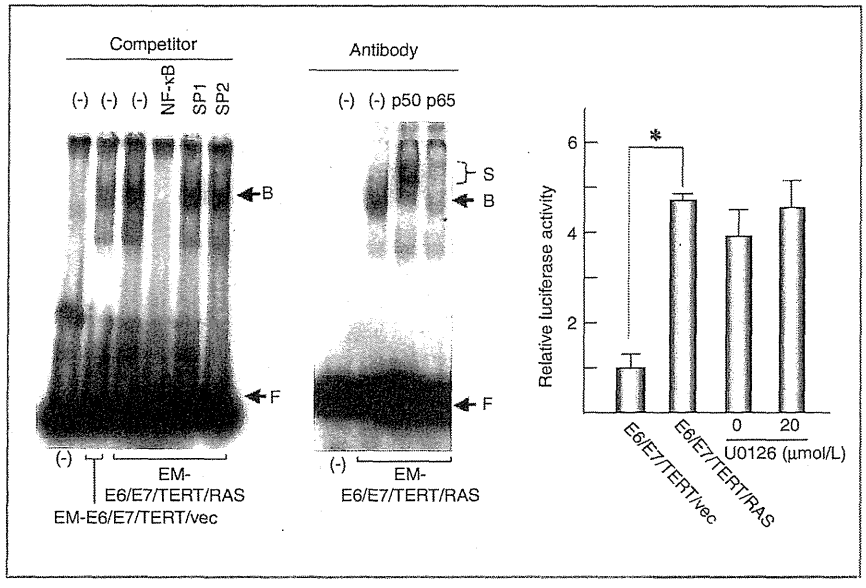

Figure 2. Oncogenic *KRAS* activates NF-κB in endometrial epithelial cells. A and B, EMSA to examine the DNA-binding activity of NF-κB. Nuclear extracts prepared from EM-E6/E7/TERT/RAS cells or the vector control EM-E6/E7/TERT/vec cells were incubated with γ^{32}-P–labeled consensus oligonucleotides containing the NF-κB–responsive elements, followed by electrophoresis. For competition assays, 100-fold molar excess of unlabeled consensus oligonucleotides for NF-κB, AP2, and SP1 were used as competitors (A). For the supershift analysis, specific antibodies against NF-κB subunit p50 or p65 were added in the reactions. B, binding complexes; F, labeled free probes; S, supershifted complexes. C, luciferase reporter assays to examine the ability of NF-κB to activate the target promoters. EM-E6/E7/TERT/RAS cells and the vector control EM-E6/E7/TERT/vec cells were transfected with luciferase reporter plasmids containing the NF-κB–responsive elements. Plates were harvested 48 hours after transfection and luciferase assays were conducted. For inhibition of the RAF-ERK pathway, 20 μmol/L of U0126 or dimethyl sulfoxide was added to the medium 6 hours after transfection. The results are presented as relative luciferase activity in which the activity from EM-E6/E7/TERT/vec cells was normalized to 1.0. Values are represented as the means of 3 independent experiments. Bars, SD. *, $P < 0.05$.

DOI:10.1158/1078-0432.CCR-10-2291

Ser36) leads to ubiquitination of IκB and subsequent proteasome-mediated degradation in the canonical NF-κB induction pathway (17). A dominant-negative mutant of IκBα, named IκBαM, has been engineered to be protected from phosphorylation and degradation. The introduction of this mutant form tightly represses the nuclear translocation and DNA binding of NF-κB (18). To elucidate the role of NF-κB in *KRAS*-induced endometrial carcinogenesis, we established cell lines with disabled NF-κB function by introducing IκBαM into EM-E6/E7/TERT/RAS cells. We first confirmed the inhibitory effect of this mutant, using the luciferase reporter assay. As shown in Figure 3A, the introduction of IκBαM significantly repressed the ability of NF-κB to activate the target promoters. We also confirmed that ERK activity was not affected by the introduction of IκBαM by Western blot analyses (Fig. 3B). Transformed phenotypes of this transfectant were evaluated by cell growth *in vitro* and the soft agar colony formation assay, tumor formation assay in nude mice, and Matrigel invasion assay. Under normal serum conditions, there was no significant increase in exponential growth rate by the introduction of IκBαM (data not shown). However, in low-serum conditions with 0.5% FBS, cells with overexpressed IκBαM exhibited decreased growth rate (Fig. 4A). We also observed that anchorage-independent growth in soft agar was almost completely abolished in these mutant cells (Fig. 4B). Furthermore, these cells completely lost their tumorigenic potential in mice (Fig. 4C). Similarly, their invasive ability significantly decreased, as evaluated by the Matrigel invasion assay (Fig. 4D). These findings indicate the crucial roles of NF-κB in *KRAS*-mediated endometrial carcinogenesis.

NF-κB activation by oncogenic *KRAS* is IKK dependent but independent of p65 phosphorylation or IκBα degradation/dissociation

We next sought to identify the molecular mechanisms of NF-κB activation by oncogenic *KRAS*. We first tested whether IKK signaling involves this activation. EM-E6/E7/TERT/RAS cells were treated with or without the IKK inhibitor X, the molecule known to inactivate IKKβ and IKKα. As shown in Figure 5A, the addition of IKK inhibitors largely inhibited the activity of NF-κB–responsive promoter in *KRAS*-introduced cells but not vector cells, indicating that this activation was IKK dependent.

Recent studies have focused on IκB subtype regulation (19) or p65 nuclear modification which can affect DNA binding and interactions with coactivators and corepressors (20, 21), Thus, we compared the basal expression levels of IκB subtypes or p65 modification between EM-E6/E7/TERT/vec and EM-E6/E7/TERT/RAS cells. As shown in Figure 5B, the expression levels of IκBα, β, ε, and p105 and those of phospho-p65 at Ser276, 529, and 536 were basically equivalent in both cells except p100. These findings suggest that IκB subtype regulation or p65 nuclear modification does not significantly contribute to *KRAS*-induced NF-κB activation during endometrial carcinogenesis.

One potential mechanism of NF-κB activation includes the degradation of IκB by its ubiquitination. Therefore, we further evaluated the change in degradation rate of IκBα by Western blot analyses, using the protein synthesis inhibitor emetine. As expected, the treatment of cells with emetine resulted in the decreased expression of IκBα in both EM-E6/E7/TERT/vec and EM-E6/E7/TERT/RAS cells but not in

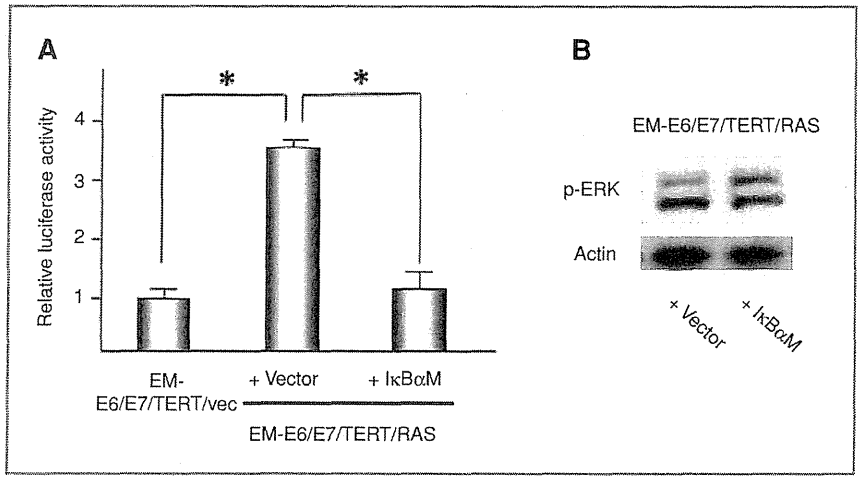

Figure 3. Introduction of IκBαM effectively inhibits NF-κB activity in transformed endometrial epithelial cells. EM-E6/E7/TERT/RAS cells were stably overexpressed with IκBαM lacking phosphorylation sites essential for its degradation, thereby becoming stable against degradation signals. Eventually, these transfectants were expected to have disabled NF-κB by IκB activity. To confirm the *in vivo* function of NF-κB in these cells, luciferase assays were done, in which EM-E6/E7/TERT/RAS cells or the vector control EM-E6/E7/TERT/vec cells were transfected with reporter plasmids containing the NF-κB–responsive elements and the luciferase assays were conducted. A, relative luciferase activities are shown as the mean values of 3 independent experiments, in which those of E6/E7/TERT/vec cells were normalized to 1.0. Bars, SD. *, $P < 0.05$. B, states of the RAF-ERK pathway were compared between EM-E6/E7/TERT/RAS cells transfected with IκBαM and the vector control cells, examining the phosphorylated ERK expression by Western blot analysis.

DOI:10.1158/1078-0432.CCR-10-2291

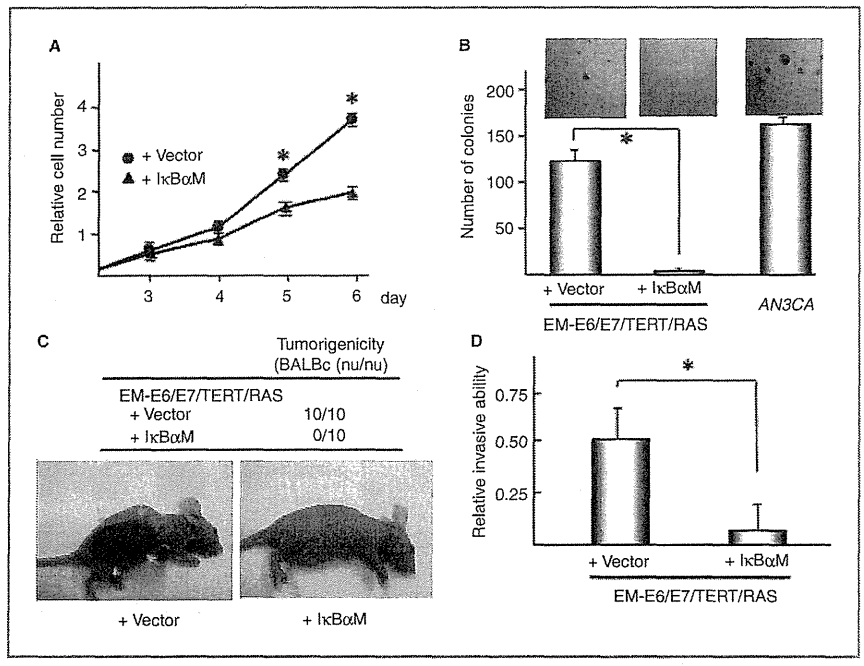

Figure 4. Transforming activity of oncogenic *KRAS* is disturbed by inhibiting NF-κB activity in endometrial epithelial cells. Transformed phenotypes of EM-E6/E7/TERT/RAS cells overexpressed with IκBαM were evaluated by various experiments. A, cell growth assay in a low-serum condition. The growth curve is shown in which EM-E6/E7/TERT/RAS cells transfected with or without IκBαM were cultured at a low-serum concentration with 0.5% FBS. Bars, SD. *, statistically significant decrease ($P < 0.05$) in the number of EM-E6/E7/TERT/RAS cells overexpressed with IκBαM compared with the number of vector control cells on days 5 and 6. B, soft agar colony formation assay. A total of 10,000 cells were seeded on soft agar in 6-cm dishes and colonies with a diameter of more than 0.05 mm 4 weeks after seeding were counted. Bars, SD. *, $P < 0.01$. C, nude mice xenograft experiment. A total of 10^7 cells of EM-E6/E7/TERT/RAS with IκBαM or control vector were inoculated subcutaneously into the right trunk of immunodeficient mice. Tumor formation was monitored for 8 weeks after inoculation. Breast cancer AN3CA cells were used as a positive control for colony formation. D, Matrigel invasion assay. EM-E6/E7/TERT/RAS cells with IκBαM or control vector were suspended in the upper wells of Matrigel chambers at 250,000 cells/chamber. After incubation, cells on the upper surface of the membrane were removed, and the cells that had migrated through the membrane to the lower surface were counted microscopically. The numbers are shown as relative invasive ability. Bars, SD. *, $P < 0.05$.

cells with overexpressed IκBαM lacking phosphorylation sites responsible for degradation (Fig. 5C). However, the degradation ratio was equivalent in EM-E6/E7/TERT/vec and EM-E6/E7/TERT/RAS cells. These results show that the activation of NF-κB by oncogenic *KRAS* is not due to accelerated degradation of IκBα.

The remaining possibility of activation mechanism might be an enhanced dissociation of p65 with IκBα (22). We tested this possibility by immunoprecipitation with p65 antibody, followed by the Western blot analysis with IκBα antibody, using extracts from EM-E6/E7/TERT/vec and EM-E6/E7/TERT/RAS cells. As shown in Figure 5D, the ratio of IκBα associated with p65 was similar between EM-E6/E7/TERT/vec and EM-E6/E7/TERT/RAS cells, denying the involvement of enhanced dissociation of p65 with IκBα.

Discussion

Using an *in vitro* carcinogenesis model with human endometrial epithelial cells, we first investigated the status of 2 major signaling pathways, the RAF-MEK-ERK and PI3K-Akt pathways, downstream of Ras. As expected, phosphorylated ERK expression significantly increased in EM-E6/E7/TERT/RAS cells (Fig. 1A). In contrast, phosphorylated Akt expression was not detected in both EM-E6/E7/TERT/vec and EM-E6/E7/TERT/RAS cells (Fig. 1B). However, the introduction of a constitutively active form of MEK, mimicking the activated RAF-MEK-ERK pathway, failed to show transformed phenotypes. Thus, activation of ERK alone was not sufficient to transform EM-E6/E7/TERT cells. There are several reports showing that constitutive activation of MEK successfully transformed rodent epithelial cells (23–26). In contrast, Boehm and colleagues showed that the introduction of a constitutively active form of MEK failed to transform immortalized human embryonic kidney epithelial cells (27). These results together with our results suggest that activation of the MEK-ERK pathway alone may not be sufficient to transform human epithelial cells and that the activation of other oncogenic pathways is required. Thus, we sought novel effectors involved in KRAS-mediated endometrial carcinogenesis.

DOI:10.1158/1078-0432.CCR-10-2291

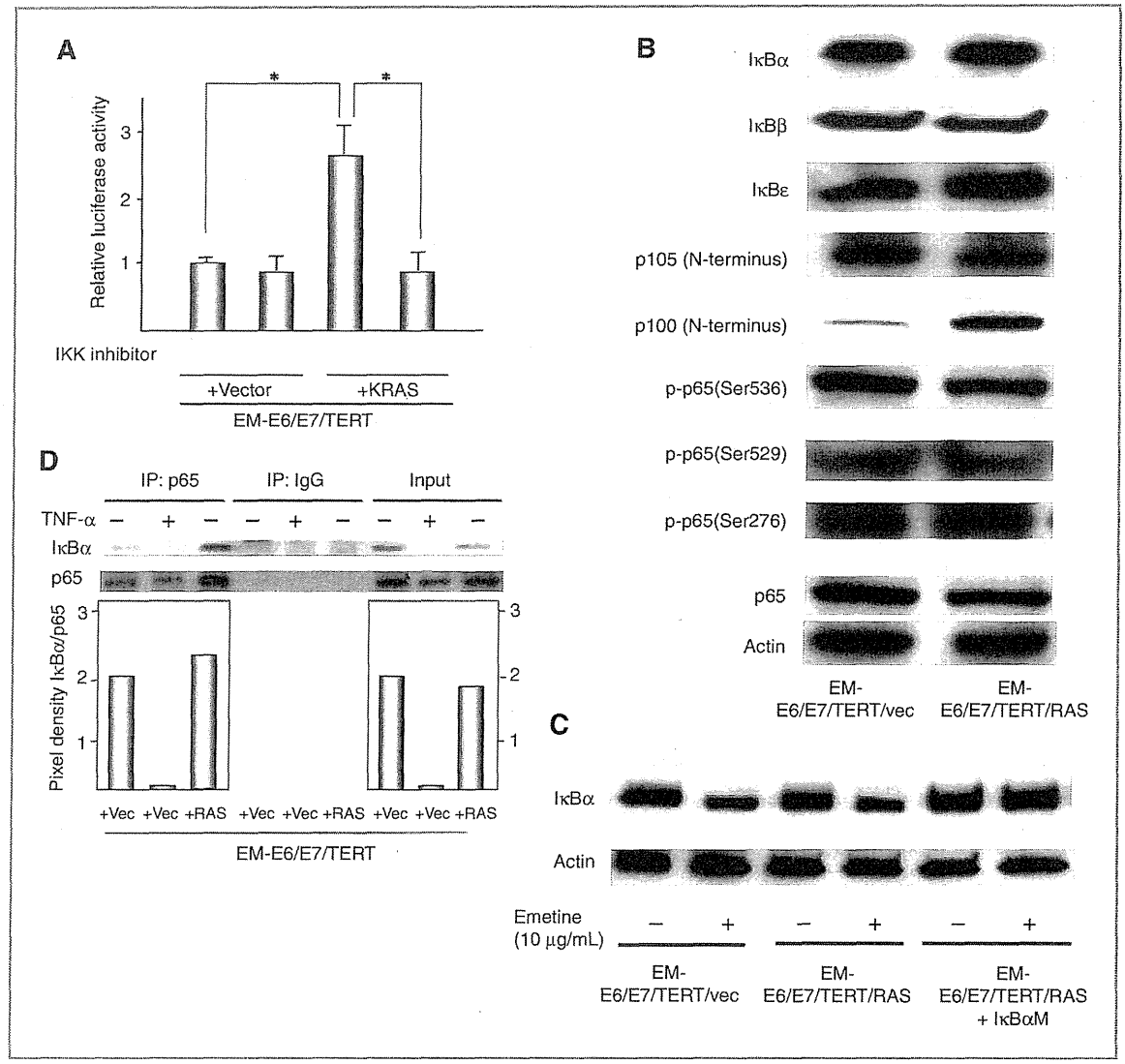

Figure 5. *KRAS*-induced activation of NF-κB in endometrial carcinogenesis is IKK dependent but not on known canonical pathways. A, IKK dependence of NF-κB activation. EM-E6/E7/TERT/vec cells or EM-E6/E7/TERT/RAS cells were transfected with reporter plasmids containing the NF-κB–responsive elements and were incubated with or without 5 μmol/L of IKK inhibitor X. Luciferase assays were carried out after 48 hours of incubation. Relative luciferase activities are shown as the mean values of 3 independent experiments, in which those of E6/E7/TERT/vec cells were normalized to 1.0. Bars, SD. *, $P < 0.05$. B, expression levels of IκB family proteins and phosphorylated p65 in *KRAS*-introduced cells. Whole-cell extracts of EM-E6/E7/TERT/vec cells or EM-E6/E7/TERT/RAS cells were subjected to the Western blot analysis, and the levels of expression in each factor are compared. C, change in IκBα turnover rate was compared between cells with or without oncogenic *KRAS*. EM-E6/E7/TERT/RAS cells or EM-E6/E7/TERT/vec cells were treated with or without 10 μg/mL of emetine and the whole-cell extracts were subjected to the Western blot analysis for IκBαM. As a control, EM-E6/E7/TERT cells with overexpressed IκBαM were used, in which IκBα level is stable even in the presence of emetine due to the lack of the specific phosphorylation site essential for degradation. D, change in dissociation rate of p65 with IκBα was compared between cells with or without oncogenic *KRAS*. Immunoprecipitation (IP) was carried out with antibodies against p65 or control IgG, using whole-cell lysates from EM-E6/E7/TERT/vec or EM-E6/E7/TERT/RAS cells. TNF-α (20 ng/mL for 5 minutes) stimulation was carried out in vector (Vec) cells to facilitate the degradation of IκBα, used as a positive control of degradation status. Western blot analysis was subsequently carried out on immunoprecipitants with antibodies to p65 or IκBα. The pixel densities of IκBα and p65 Western blots were quantified using NIH Scion software. Graph represents the relative pixel density of IκBα normalized to p65 levels in each sample.

DOI:10.1158/1078-0432.CCR-10-2291

NF-κB transcriptional factor is a putative effector of Ras-mediated transformation (8–10). We showed that oncogenic *KRAS* enhanced the NF-κB binding to its responsive elements and facilitated the transactivation of the target promoters. The introduction of IκBαM successfully inhibited transactivation of NF-κB without affecting ERK activity, and we found that such inhibition completely abrogated the anchorage-independent growth and tumor-forming ability of EM-E6/E7/TERT/RAS cells, suggesting a major contribution of NF-κB activity to *KRAS*-induced carcinogenesis of endometrial epithelial cells.

What is the molecular mechanism of NF-κB activation in *KRAS*-induced endometrial carcinogenesis? The transactivation of promoters by NF-κB is directly controlled by its nuclear translocation and its modification in the nucleus. In most cell types, NF-κB dimers are sequestered in the cytoplasm and inactivated by IκB proteins, which bind to the NF-κB and mask the nuclear localization signal (28). The phosphorylation of a specific serine residue, Ser32/36, in IκBα by the upstream regulators such as IKK results in polyubiquitination and subsequent degradation by 26 S proteasomes, causing release of the NF-κB dimer and promoting its translocation to the nucleus, activating various κB-responsive gene expressions (29, 30). Thus, we first tested the involvement of IKK in the activation. The treatment of EM-E6/E7/TERT/RAS cells with the IKK inhibitor X significantly suppressed NF-κB transcriptional activity, confirming that *KRAS*-induced NF-κB activation was IKK dependent. We further examined the basal expression levels of IκB family proteins in the presence or absence of oncogenic *KRAS* and found that the expression levels of IκB proteins, including IκBα, β, ε, and p105, were not affected by oncogenic *KRAS*. Expression of p100 protein, which is a member of the IκB protein family and a precursor of NF-κB subunit p52 (31), increased in EM-E6/E7/TERT/RAS cells. This is probably because the p100 promoter contains a κB site (32). We do not consider that this phenomenon is involved in NF-κB activation, because the increased expression of p100 may inhibit NF-κB activity but never activates NF-κB. In addition, the expression of p52 was unchanged (data not shown). Therefore, we speculate that the p100/p52 subunit is not likely to participate in NF-κB activation by oncogenic *KRAS*. Furthermore, we focused on the modification of the NF-κB subunit itself. Nuclear NF-κB modification, especially p65/RelA subunit modification, has been investigated and found to affect DNA binding and interactions with coactivators and corepressors and the termination of the NF-κB response (33). These modifications include phosphorylation of Ser536 and Ser529 in the C-terminal transactivation domains and Ser276 in the Rel homology domain (17, 34–36). However, the expression of phosphorylated p65 was not elevated in the *KRAS*-introduced cells. We further confirmed the possibility of increased IκB degradation that might result in NF-κB activation. The IκB turnover assay with protein synthesis inhibitor revealed that the turnover was not accelerated by oncogenic *KRAS*, again denying the possibility as an activation mechanism. Recently proven additional mechanisms of NF-κB activation is a dissociation of IκB from p65 in the absence of IκB degradation (22, 37). We examined the interaction of IκBα and p65 by immunoprecipitation. The expression levels of IκBα attached to p65 was, however, equivalent between EM-E6/E7/TERT/vec and EM-E6/E7/TERT/RAS cells, showing that such dissociation is not involved in *KRAS*-mediated NF-κB activation. Thus, we concluded that *KRAS*-induced activation of NF-κB during endometrial carcinogenesis is IKK dependent but not on known canonical pathways. Identification of such unknown mechanisms is needed using our model for understanding not only of the activation mechanisms of NF-κB but also of the carcinogenesis of endometrium.

So far, only one study has addressed *KRAS* mutation and NF-κB activation in endometrial cancer (38). This report examined surgically resected cancer tissues and reported the high frequency of nuclear location of NF-κB families. However, no correlation was found between the nuclear immunostaining of NF-κB and *KRAS* mutation. These findings do not conflict with our results, because their analyses were carried out using specimens of progressive cancers and not samples at the stage of cancer initiation or development, in which network of etiologic factors might be modified because of acquired genetic alterations during the late stage of cancer development.

This study may provide a clinical implication for NF-κB as a novel molecular target for cancer chemoprevention of the endometrium. Accumulating evidence has clarified chemopreventive effects of anti-inflammatory agents such as aspirin or other nonsteroidal anti-inflammatory drugs on various cancer types partially via inhibition of NF-κB (39, 40). As for endometrial cancer, Moysich and colleagues reported the risk reduction by regular use of aspirin among obese women (41). Interestingly, multiple signaling pathways, including PTEN-PI3K-Akt pathway, are known to activate NF-κB in endometrial cancer cells (42). Loss of function mutation in *PTEN* and activating mutation in *PIK3CA* are putative activator of NF-κB through Akt expression in endometrial cancer and in the precursor lesions (43). Therefore, it is possible that NF-κB plays a role in endometrial carcinogenesis via various pathways other than *KRAS*-driven pathways, giving light to the potential role of NF-κB inhibitors in preventing endometrial carcinogenesis.

In summary, we for the first time show that the activation of NF-κB is a novel target of oncogenic *KRAS* in endometrial carcinogenesis. Blockade of NF-κB activity led to effective inhibition of transformed phenotypes of endometrial cells. These findings may add the novel information on the molecular pathway of endometrial carcinogenesis, implying the potential utility of NF-κB inhibitors for endometrial cancer chemoprevention, especi'ally with *KRAS* mutation.

Disclosure of Potential Conflicts of Interest

The authors declare no conflict of interest.

DOI:10.1158/1078-0432.CCR-10-2291

Grant Support

This study was supported by a grant-in-aid for Scientific Research from the Japan Society for the Promotion of Science (JSPS) and the Megumi Medical Foundation of Kanazawa University.

The costs of publication of this article were defrayed in part by the payment of page charges. This article must therefore be hereby marked *advertisement* in accordance with 18 U.S.C. Section 1734 solely to indicate this fact.

Received August 26, 2010; revised December 17, 2010; accepted December 29, 2010; published online March 16, 2011.

References

1. Hecht JL, Mutter GL. Molecular and pathologic aspects of endometrial carcinogenesis. J Clin Oncol 2006;24:4783–91.
2. Inoue M. Current molecular aspects of the carcinogenesis of the uterine endometrium. Int J Gynecol Cancer 2001;11:339–48.
3. Enomoto T, Inoue M, Perantoni AO, Buzard GS, Miki H, Tanizawa O, et al. K-ras activation in premalignant and malignant epithelial lesions of the human uterus. Cancer Res 1991;51:5308–14.
4. Mutter GL. K-ras mutations appear in the premalignant phase of both microsatellite stable and unstable endometrial carcinogenesis. Mol Pathol 1999;52:257–62.
5. Shields JM, Pruitt K, McFall A, Shaub A, Der CJ. Understanding Ras: "it ain't over 'til it's over." Trends Cell Biol 2000;10:147–54.
6. Kyo S, Nakamura M, Kiyono T, Maida Y, Kanaya T, Tanaka M, et al. Successful immortalization of endometrial glandular cells with normal structural and functional characteristics. Am J Pathol 2003;163:2259–69.
7. Mizumoto Y, Kyo S, Ohno S, Hashimoto M, Nakamura M, Maida Y, et al. Creation of tumorigenic human endometrial epithelial cells with intact chromosomes by introducing defined genetic elements. Oncogene 2006;25:5673–82.
8. Bassères DS, Baldwin AS. Nuclear factor-kappaB and inhibitor of kappaB kinase pathways in oncogenic initiation and progression. Oncogene 2006;25:6817–30.
9. Hanson JL, Hawke NA, Kashatus D, Baldwin AS. The nuclear factor kappaB subunits RelA/p65 and c-Rel potentiate but are not required for Ras-induced cellular transformation. Cancer Res 2004;64:7248–55.
10. Arsura M, Mercurio F, Oliver AL, Thorgeirsson SS, Sonenshein GE. Role of the IkappaB kinase complex in oncogenic Ras- and Raf-mediated transformation of rat liver epithelial cells. Mol Cell Biol 2000;20:5381–91.
11. Millán O, Ballester A, Castrillo A, Oliva JL, Través PG, Rojas JM, et al. H-Ras-specific activation of NF-kappaB protects NIH 3T3 cells against stimulus-dependent apoptosis. Oncogene 2003;22:477–83.
12. Schreiber E, Matthias P, Müller MM, Schaffner W. Rapid detection of octamer binding proteins with "mini-extracts," prepared from a small number of cells. Nucleic Acids Res 1989;17:6419.
13. Gopalbhai K, Jansen G, Beauregard G, Whiteway M, Dumas F, Wu C, et al. Negative regulation of MAPKK by phosphorylation of a conserved serine residue equivalent to Ser212 of MEK1. J Biol Chem 2003;278:8118–25.
14. Narisawa-Saito M, Yoshimatsu Y, Ohno S, Yugawa T, Egawa N, Fujita M, et al. An *in vitro* multistep carcinogenesis model for human cervical cancer. Cancer Res 2008;68:5699–705.
15. Sato H, Takino T, Okada Y, Cao J, Shinagawa A, Yamamoto E, et al. A matrix metalloproteinase expressed on the surface of invasive tumour cells. Nature 1994;370:61–5.
16. Brunet A, Pagès G, Pouysségur J. Constitutively active mutants of MAP kinase kinase (MEK1) induce growth factor-relaxation and oncogenicity when expressed in fibroblasts. Oncogene 1994;9:3379–87.
17. DiDonato J, Mercurio F, Rosette C, Wu-Li J, Suyang H, Ghosh S, et al. Mapping of the inducible IkappaB phosphorylation sites that signal its ubiquitination and degradation. Mol Cell Biol 1996;16:1295–304.
18. Wang CY, Mayo MW, Baldwin AS Jr. TNF- and cancer therapy-induced apoptosis: potentiation by inhibition of NF-kappaB. Science 1996;274:784–7.
19. Hayden MS, Ghosh S. Signaling of NF-kappaB. Genes Dev 2004;18:2195–224.
20. Vermeulen L, De Wilde G, Van Damme P, Vanden Berghe W, Haegeman G. Transcriptional activation of the NF-kappaB p65 subunit by mitogen- and stress-activated protein kinase-1 (MSK1). EMBO J 2003;22:1313–24.
21. Chen LF, Williams SA, Mu Y, Nakano H, Duerr JM, Buckbinder L, et al. NF-kappaB RelA phosphorylation regulates RelA acetylation. Mol Cell Biol 2005;25:7966–75.
22. Sitcheran R, Comb WC, Cogswell PC, Baldwin AS. Essential role for epidermal growth factor receptor in glutamate receptor signaling to NF-kappaB. Mol Cell Biol 2008;28:5061–70.
23. Haluska FG, Tsao H, Wu H, Haluska FS, Lazar A, Goel V. Genetic alterations in signaling pathways in melanoma. Clin Cancer Res 2006;12:2301s–7s.
24. Deerberg F, Kaspareit J. Endometrial carcinoma in BD II/Han rats: model of a spontaneous hormone-dependent tumor. J Natl Cancer Inst 1987;78:1245–51.
25. Komatsu K, Buchanan FG, Otaka M, Jin M, Odashima M, Horikawa Y, et al. Gene expression profiling following constitutive activation of MEK1 and transformation of rat intestinal epithelial cells. Mol Cancer 2006;5:63.
26. Pinkas J, Leder P. MEK1 signaling mediates transformation and metastasis of EpH4 mammary epithelial cells independent of an epithelial to mesenchymal transition. Cancer Res 2002;62:4781–90.
27. Boehm JS, Zhao JJ, Yao J, Kim SY, Firestein R, Dunn IF, et al. Integrative genomic approaches identify IKBKE as a breast cancer oncogene. Cell 2007;129:1065–79.
28. Huxford T, Huang DB, Malek S, Ghosh G. The crystal structure of the IkappaBalpha/NF-kappaB complex reveals mechanisms of NF-kappaB inactivation. Cell 1998;95:759–70.
29. Chen Z, Hagler J, Palombella VJ, Melandri F, Scherer D, Ballard D, et al. Signal-induced site-specific phosphorylation targets I kappa B alpha to the ubiquitin-proteasome pathway. Genes Dev 1995;9:1586–97.
30. Scherer DC, Brockman JA, Chen Z, Maniatis T, Ballard DW. Signal-induced degradation of I kappa B alpha requires site-specific ubiquitination. Proc Natl Acad Sci U S A 1995;92:11259–63.
31. Dejardin E. The alternative NF-kappaB pathway from biochemistry to biology: pitfalls and promises for future drug development. Biochem Pharmacol 2006;72:1161–79.
32. Lombardi L, Ciana P, Cappellini C, Trecca D, Guerrini L, Migliazza A, et al. Structural and functional characterization of the promoter regions of the NFKB2 gene. Nucleic Acids Res 1995;23:2328–36.
33. Perkins ND. Post-translational modifications regulating the activity and function of the nuclear factor kappa B pathway. Oncogene 2006;25:6717–30.
34. Sakurai H, Chiba H, Miyoshi H, Sugita T, Toriumi W. IkappaB kinases phosphorylate NF-kappaB p65 subunit on serine 536 in the transactivation domain. J Biol Chem 1999;274:30353–6.
35. Zhong H, Voll RE, Ghosh S. Phosphorylation of NF-kappa B p65 by PKA stimulates transcriptional activity by promoting a novel bivalent interaction with the coactivator CBP/p300. Mol Cell 1998;1:661–71.
36. Wang D, Westerheide SD, Hanson JL, Baldwin AS Jr. Tumor necrosis factor alpha-induced phosphorylation of RelA/p65 on Ser529 is controlled by casein kinase II. J Biol Chem 2000;275:32592–7.
37. Mabuchi R, Sasazuki T, Shirasawa S. Mapping of the critical region of mitogene-inducible gene-6 for NF-kappaB activation. Oncol Rep 2005;13:473–6.

DOI:10.1158/1078-0432.CCR-10-2291

38. Pallares J, Martínez-Guitarte JL, Dolcet X, Llobet D, Rue M, Palacios J, et al. Abnormalities in the NF-kappaB family and related proteins in endometrial carcinoma. J Pathol 2004;204:569–77.
39. Cuzick J, Otto F, Baron JA, Brown PH, Burn J, Greenwald P, et al. Aspirin and non-steroidal anti-inflammatory drugs for cancer prevention: an international consensus statement. Lancet Oncol 2009;10:501–7.
40. Zhang Z, Rigas B. NF-kappaB, inflammation and pancreatic carcinogenesis: NF-kappaB as a chemoprevention target. Int J Oncol 2006;29:185–92.
41. Moysich KB, Baker JA, Rodabaugh KJ, Villella JA. Regular analgesic use and risk of endometrial cancer. Cancer Epidemiol Biomarkers Prev 2005;14:2923–8.
42. St-Germain ME, Gagnon V, Parent S, Asselin E. Regulation of COX-2 protein expression by Akt in endometrial cancer cells is mediated through NF-kappaB/IkappaB pathway. Mol Cancer 2004;3:7.
43. Hayes MP, Wang H, Esponal-Witter R. PIK3CA and PTEN mutation in uterine endometrioid carcinoma and complex hyperplasia. Clin Cancer Res 2006;12:5932–5.

JOURNAL OF VIROLOGY, Nov. 2010, p. 11614–11623 Vol. 84, No. 22
0022-538X/10/$12.00 doi:10.1128/JVI.01053-10

CD1d, a Sentinel Molecule Bridging Innate and Adaptive Immunity, Is Downregulated by the Human Papillomavirus (HPV) E5 Protein: a Possible Mechanism for Immune Evasion by HPV▽

Shiho Miura,[1] Kei Kawana,[1]* Danny J. Schust,[2] Tomoyuki Fujii,[1] Terufumi Yokoyama,[3] Yuki Iwasawa,[1] Takeshi Nagamatsu,[1] Katsuyuki Adachi,[1] Ayako Tomio,[1] Kensuke Tomio,[1] Satoko Kojima,[1] Toshiharu Yasugi,[1] Shiro Kozuma,[1] and Yuji Taketani[1]

Department of Obstetrics and Gynecology, Faculty of Medicine, University of Tokyo, 7-3-1 Hongo, Bunkyo-ku, Tokyo 113-8655, Japan[1]; Division of Reproductive Endocrinology and Fertility, Department of Obstetrics, Gynecology, and Women's Health, University of Missouri School of Medicine, Columbia Regional Hospital, 402 Keene Street, Third Floor, Columbia, Missouri 65201[2]; and GENOLAC BL Corp. 503, Okinawa Industry Support Center, 1831-1, Oroku, Naha, Okinawa 901-0152, Japan[3]

Received 16 May 2010/Accepted 20 August 2010

CD1d and CD1d-restricted natural killer T (NKT) cells serve as a natural bridge between innate and adaptive immune responses to microbes. CD1d downregulation is utilized by a variety of microbes to evade immune detection. We demonstrate here that CD1d is downregulated in human papillomavirus (HPV)-positive cells *in vivo* and *in vitro*. CD1d immunoreactivity was strong in HPV-negative normal cervical epithelium but absent in HPV16-positive CIN1 and HPV6-positive condyloma lesions. We used two cell lines for *in vitro* assay; one was stably CD1d-transfected cells established from an HPV-negative cervical cancer cell line, C33A (C33A/CD1d), and the other was normal human vaginal keratinocyte bearing endogenous CD1d (Vag). Flow cytometry revealed that cell surface CD1d was downregulated in both C33A/CD1d and Vag cells stably transfected with HPV6 E5 and HPV16 E5. Although the steady-state levels of CD1d protein decreased in both E5-expressing cell lines compared to empty retrovirus-infected cells, CD1d mRNA levels were not affected. Confocal microscopy demonstrated that residual CD1d was not trafficked to the E5-expressing cell surface but colocalized with E5 near the endoplasmic reticulum (ER). In the ER, E5 interacted with calnexin, an ER chaperone known to mediate folding of CD1d. CD1d protein levels were rescued by the proteasome inhibitor, MG132, indicating a role for proteasome-mediated degradation in HPV-associated CD1d downregulation. Taken together, our data suggest that E5 targets CD1d to the cytosolic proteolytic pathway by inhibiting calnexin-related CD1d trafficking. Finally, CD1d-mediated production of interleukin-12 from the C33A/CD1d cells was abrogated in both E5-expressing cell lines. Decreased CD1d expression in the presence of HPV E5 may help HPV-infected cells evade protective immunological surveillance.

There are approximately 100 identified genotypes (types) of human papillomavirus (HPV). Over 40 of these are classified as genital HPV subtypes that invade the reproductive organs, including the uterine cervix, vaginal wall, vulva, and penis. Genital HPV types are further subclassified into high-risk types that are commonly associated with cervical cancer and low-risk types that cause noninvasive condyloma acuminata. Although exact classification varies among researchers, subtypes 16, 18, 31, 33, 35, 39, 45, 51, 52, 56, 58, 66, and 68 are typically classified as high risk and subtypes 6, 11, 40, 42, 43, 44, 54, 61, and 72 as low risk (44). Genital HPV infection involves short-term virus proliferation, followed by the long-term latent presence of a small number of copies of the viral genome within the basal cells of the genital epithelium (44). Infections with high-risk HPV subtypes result in progression to genital tract cancers (most commonly cervical) in only a small percentage of infected women and typically after a long latency period. A high percentage of high-risk HPV DNA-positive infected women resolve their infections during the proliferative phase and thereby clear the virus or progress to latency with undetectable HPV DNA levels. The clearance of viral DNA is often accomplished through activation of the host immune system against viral antigen (19), and chronic immune suppression represents a risk factor for viral DNA persistence and benign and/or neoplastic lesion progression (23).

Completion of the HPV life cycle requires infection of epidermal or mucosal basal cells that have the potential to proliferate and differentiate. Within these cells, overall viral gene expression is suppressed, although limited expression of specific early viral genes, including E5, E6, and E7, causes lateral expansion of infected cells within the basal layer of the epithelium (44). HPV E5 seems to be particularly important early in the course of infection. Large amounts of E5 mRNA have been found in cervical intraepithelial neoplasia (CIN) lesions (37). However, as HPV-infected lesions progress to cervical cancer, episomal viral DNA becomes integrated into host cell DNA, and a substantial part of the HPV genome, commonly including the E5 coding sequence, is deleted (16). Therefore, E5 is not obligatory in the late events of HPV-mediated carcinogenesis.

E5 is a small hydrophobic protein that can be localized within the Golgi apparatus (GA), endoplasmic reticulum

* Corresponding author. Mailing address: Department of Obstetrics and Gynecology, Faculty of Medicine, University of Tokyo, 7-3-1 Hongo, Bunkyo-ku, Tokyo 113-8655, Japan. Phone: 81-3-3815-5411. Fax: 81-3-3816-2017. E-mail: kkawana-tky@umin.ac.jp.

▽ Published ahead of print on 1 September 2010.

(ER), and occasionally at the plasma membrane of the host cell. It has been proposed that binding of HPV16 E5 to a subunit of the cellular proton ATPase (15) is responsible for the lack of acidification of the GA and endolysosomes and the consequent impaired function of these organelles that is seen with HPV16 infection (32, 38). The presence of HPV16 E5 has also been linked to downregulation of antigen presentation by HLA class I molecules, a process that may aid in HPVs ability to evade immune clearance through cytotoxic-T-lymphocyte (CTL)-mediated adaptive immunity (1, 2, 3, 21, 30). Ashrafi and coworkers have demonstrated that HPV16 E5 retains HLA-A and -B molecules in the GA and interferes with their trafficking to the cell surface but does not alter the transcription of HLA class I heavy chains or the transporter associated with antigen processing (TAP) (2, 3, 4, 28). Others have shown that HPV16 E5 interacts with calnexin in the ER and thereby interferes with the modification of HLA class I heavy chains (21).

CD1d is an major histocompatibility complex (MHC) class I-like glycoprotein that presents self or microbial lipid antigen to natural killer T (NKT) cells (39). In humans, a specific subset of NKT cells expresses an invariant Vα24-JaQ/Vβ11 TCR (iTCR) and can recognize CD1d on the surface of antigen-presenting cells (APCs) through this receptor. CD1d is expressed not only in typical APCs (macrophages, dendritic cells, and B cells) but also in intestinal epithelial cells (8, 12), foreskin keratinocytes (9), and reproductive tract epithelial cells (25, 26). Like MHC class I, CD1d is synthesized, glycosylated by *N*-glycosyltransferase, modified, and assembled with β2m within the ER and then transferred to the GA (5, 24, 27). CD1d plays a role in both innate and adaptive immunity to various bacteria, viruses, fungi, and parasites (reviewed in reference 10). Activation of CD1d-restricted invariant NKT (iNKT) cells enhances host resistance to some microbes in a manner that depends on the level of CD1d expression on APCs (34, 35). In contrast, the activation of iNKT cells promotes susceptibility to some microbes (7, 33). The activation of CD1d-restricted iNKT cells in response to microbial invasion is antigen dependent, but these antigens can be derived from the invading microbe or possibly from host lipids (11, 22, 29). Intracellular signaling mediated by surface CD1d utilizes NF-κB, a well-known immune-related transcription factor (36, 43). CD1d-restricted NKT cells can modulate adaptive immune cells by altering Th1/Th2 polarization. Recognition of CD1d by iNKT cells can also result in rapid release of both interleukin-4 (IL-4) and gamma interferon (IFN-γ) from the NKT cell (6). Therefore, CD1d and CD1d-restricted NKT cells serve as a natural bridge between innate and adaptive immune responses to microbes. Not surprisingly, several microbes, including herpes simplex virus type 1, human immunodeficiency virus, Kaposi's sarcoma herpesvirus, and *Chlamydia trachomatis*, are known to downregulate cell surface expression of CD1d as an immune evasion strategy (13, 26, 31, 42). Our own lab previously demonstrated that *C. trachomatis* retains CD1d in the ER and targets CD1d to both chlamydial and cellular degradation pathways (26).

Viewing the importance of CD1d in innate immune responses to microbes, we hypothesized that HPV may alter CD1d-mediated immune pathways and thereby avoid innate immune destruction of the infected cell by the host. We demonstrate here that the presence of the E5 protein of HPV6 and HPV16 is associated with reduced CD1d cell surface expression. We describe a mechanism for this downregulation and hypothesize that decreased surface CD1d expression may help HPV-infected cells evade immune surveillance during the early stages of infection.

MATERIALS AND METHODS

HPV6 and HPV16 E5 expression constructs. HPV6 and HPV16 E5 open reading frames were amplified from the HPV6 and HPV16 complete genomes (kindly provided by Tadahito Kanda, National Institute of Infectious Diseases, Japan) by PCR using primers designed to introduce BamHI (forward) and EcoRI (reverse) restriction sites. The PCR products were digested with BamHI and EcoRI and subcloned into a retroviral expression plasmid pLPCX (Clontech, Mountain View, CA).

Cell lines and establishment of a cell line stably expressing CD1d. An HPV-negative human cervical carcinoma cell line, C33A, and a vaginal epithelial cell that was originally established from normal human primary epithelial cells that were immortalized by transduction with HPV16 E6/E7 genes (VK2/E6E7) (a generous gift from D. J. Anderson, Boston University, Boston, MA) (18) were grown in Dulbecco modified eagle medium (Invitrogen, Carlsbad, CA) without $CaCl_2$ (Invitrogen), supplemented with 10% fetal bovine serum (Invitrogen) at 37°C in 5% CO_2. The vaginal epithelial (VK2/E6E7) cells used here are known to express endogenous CD1d at the cell surface (25).

A CD1d-expressing retroviral plasmid pSRα-neo (kindly provided by R. Blumberg, Harvard Medical School, Boston, MA) was transfected into Phoenix cells, a packaging cell line for recombinant retroviruses (kindly provided by K. Oda, University of Tokyo), using Lipofectamine 2000 (Invitrogen). After 72 h of incubation in DMEM, the culture medium containing released CD1d-expressing retroviruses was collected and used to infect C33A cells and transfer the CD1d gene. CD1d-expressing C33A cells were selected in medium containing 1.0 mg of neomycin/ml to establish a stably transfected cell line (C33A/CD1d).

Establishment of HPV E5-expressing cell lines. HPV6 or HPV16 E5-expressing retroviral plasmids or their empty counterparts (pLPCX-16E5, pLPCX-6E5, or pLPCX, respectively) were transfected into Phoenix cells using Lipofectamine 2000 (Invitrogen). After 72 h of incubation, culture medium with released viruses were collected and used to infect C33A/CD1d or vaginal epithelial cells. Stable cell lines were selected in media containing 1.5 μg of piromycin/ml.

Immunohistochemistry. Immunostaining for CD1d was performed on formalin-fixed, paraffin-embedded tissue sections of normal or inflamed cervix, CIN1 to CIN3, cervical cancer, and condyloma acuminata (obtained under IRB approval through the University of Tokyo). A total of 45 tissues were examined. Optimal immunostaining required antigen retrieval via microwave exposure in 0.01 M citrate buffer. A mouse anti-CD1d MAb (NOR3.2, 1:100; Abcam, Inc., Cambridge, MA) or an irrelevant, isotype-matched mouse monoclonal antibody (DakoCytomation, Glostrup, Denmark) were used as primary reagents. Immunostaining was amplified and detected by using the EnVision+System-HRP (DakoCytomation). Nuclei were counterstained by using standard hematoxylin protocols (Sigma-Aldrich, Inc., St. Louis, MO). Analyses were performed at a magnification of ×200.

Flow cytometry. C33A/CD1d cells were grown in 175-cm^2 flasks until confluent, harvested using trypsin-EDTA, and pelleted at 500 × *g* for 5 min at room temperature. The cells were then washed and resuspended in PBS-B (phosphate-buffered saline [PBS] with 1% bovine serum albumin; Invitrogen) at a concentration of 10^6 cells/ml. For detection of cell surface CD1d, 100 μl of cell suspension was incubated with an anti-CD1d NOR3.2 monoclonal antibody (MAb; Abcam) at 1:100 for 30 min at 4°C. Cells were then washed three times in PBS-B, incubated with a goat anti-mouse immunoglobulin secondary antibody conjugated to phycoerythrin (PE; BD Bioscience, San Jose, CA) for 30 min at 4°C, suspended in 1% paraformaldehyde, and analyzed by using a FACSCalibur flow cytometry system (BD Bioscience).

Proteasome inhibitor treatment. C33A/CD1d cells harboring an empty vector (C33A/CD1d-empty) or expressing HPV6 E5 (C33A/CD1d-6E5) or HPV16 E5 (C33A/CD1d-16E5) were cultured for up to 24 h in the presence or absence of the cytosolic proteasome inhibitor MG132 (10 μM in dimethyl sulfoxide [DMSO]; Sigma-Aldrich, Inc.). Control wells included vehicle alone.

HPV genotyping. DNA was extracted from cervical smear samples by using the DNeasy blood minikit (Qiagen, United Kingdom). HPV genotyping was performed by using the PGMY-CHUV assay method (20). Briefly, standard PCR was conducted using the PGMY09/11 L1 consensus primer set and HLA-dQ primer sets (20). Reverse blotting hybridization was performed as described

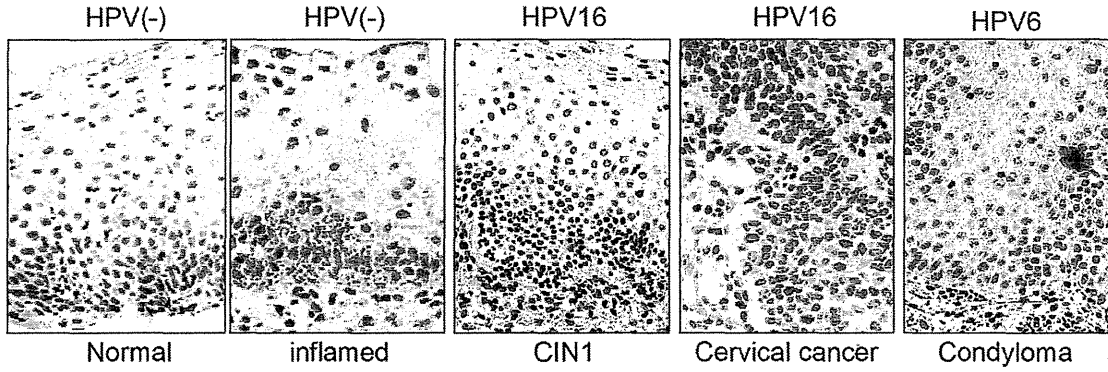

FIG. 1. Immunostaining of HPV-associated lesions for CD1d. Immunostaining for CD1d was performed after antigen retrieval on formalin-fixed, paraffin-embedded tissue sections of HPV-negative normal and inflamed ectocervical epithelium, HPV16-positive CIN1, HPV16-positive cervical cancer, and HPV6-positive condyloma acuminata. CD1d was detected with NOR3.2, a CD1d-specific MAb (1:100).

previously (20). Heat-denatured PCR amplicons were hybridized to a negatively charged nylon membrane containing specific probes for 32 HPV genotypes and HLA-dQ reference samples. Chemiluminescence detection used enhanced chemiluminescence (ECL) detection reagents for nucleic acids (GE Healthcare). Films were interpreted using the HPV reference guide provided.

RT-PCR and quantitative PCR. Portions (1 μg) of total RNA and oligo(dT)s were used for reverse transcriptase (RT) reactions (RNA PCR kit; Applied Biosystems, Foster City, CA). Total cDNA reaction samples were used as templates for amplification of each gene fragment using a PCR Core kit (Applied Biosystems). Primer pair sets for CD1d were synthesized by Invitrogen (CD1d, 453 bp; 5′-GCTGCAACCAGGACAAGTGGACGAG-3′ [forward] and 5′-AGGAACAGCAAGCACGCCAGGACT-3′ [reverse]). Those for IL-12 p40 were commercially available (Sigma-Aldrich, Inc.). For quantitative PCR, cDNA were produced via RT of 1 μg of total RNA extracted from the cells as described above by using an OmniScript RT kit (Qiagen, Inc., Valencia, CA). Portions (2 μl) of 5-fold-diluted cDNA aliquots were amplified in a thermal cycler (7300 Real-Time PCR System; Applied Biosystems) by using a QuantiTect SYBR green PCR kit (Qiagen, Inc.) and a primer pair set for β-actin (5′-GAAATCGTGCGTGACATTAAGG-3′[forward] and 5′-TCAGGCAGCTCGTAGCTTCT-3′ [reverse]). The mRNA levels for IL-12 were normalized to those of β-actin, the internal control.

Fluorescent deconvolution microscopy and confocal microscopy. C33A/CD1d cells were seeded onto coverslips. The ER was visualized using the ER tracker Blue-White DPX (Invitrogen) for 30 min at 37°C. All coverslips were fixed in 4% paraformaldehyde, permeabilized with 0.1% Tween 20. They were then incubated for 1 h at 37°C with either an anti-CD1d NOR3.2 MAb labeled with Zenon Alexa Fluor 555 using a mouse IgG labeling kit (Invitrogen) or an anti-FLAG MAb labeled with Zenon Alexa Fluor 488 using a mouse IgG labeling kit (Invitrogen) singly or in combination. With the exception of ER tracker-treated coverslips, the cells were then counterstained with a DAPI (4′,6′-diamidino-2-phenylindole) nucleic acid stain (Invitrogen). Images were obtained with a LSM 700, flexible confocal microscope (Carl Zeiss, Oberkochen, Germany). Filter sets were optimized for Alexa 488, Alexa 555, and DAPI. Z-axis plane capture, deconvolution, and analyses were performed with ZEN 2009 Software (Carl Zeiss).

Western blotting. Portions (50 μg) of total cell lysates from C33A/CD1d-empty, C33A/CD1d-6E5, or C33A/CD1d-16E5 cells in a modified TNF buffer (1 M Tris-HCl [pH 7.8], 10% NP-40, 5 M NaCl, 0.5 M EDTA [pH 8.0], aprotinin, 0.1 M phenylmethylsulfonyl fluoride) were electrophoresed and transferred to nitrocellulose membranes. Membranes were blocked with 10% milk and incubated with a peroxidase-labeled anti-CD1d NOR3.2 MAb (1:200; Abcam) or an anti-FLAG MAb (1:500; Sigma-Aldrich, Inc.) using a peroxidase labeling kit (Roche, Basel, Switzerland) for 1 h. Membranes were washed and bound antibody was detected using an ECL Western blotting analysis system (GE Healthcare Buckinghamshire, United Kingdom).

Immunoprecipitation and Western immunoblotting. Harvested C33A/CD1d-empty, C33A/CD1d-6E5, or C33A/CD1d-16E5 cells were lysed in modified radioimmunoprecipitation assay buffer (1% NP-40, 1% deoxycholate, 0.1% sodium dodecyl sulfate [SDS], 10 mM Tris, 150 mM NaCl, 2 mM EDTA) with protease inhibitors (Amersham Biosciences, Piscataway, NJ). Equivalent aliquots of total cell lysates were incubated overnight at 4C with 5 μg of mouse anti-FLAG MAbs (Sigma-Aldrich, Inc.)/ml and 5 μl of protein A-Sepharose (GE Healthcare). Precipitated proteins were separated by SDS-PAGE using 7.5% acrylamide gels and transferred to polyvinylidene difluoride membranes. Mouse anti-calnexin or rabbit anti-β-actin polyclonal antibodies (Abcam) were used as primary reagents for immunoblotting, and anti-mouse IgG-HRP (1:100,000; GE Healthcare) was used as a secondary reagent. Products in Western immunoblotting experiments were visualized by using an ECL Western blotting analysis system (GE Healthcare). Molecular masses were confirmed by comparison to standard size markers (GE Healthcare).

Statistical analysis. Quantitative PCR data were presented as means ± the standard deviations. Experiments were performed independently at least three times. The Cochran-Armitage Trend test was computed to show trends in immune reactivity with NOR3.2 MAb in clinical samples. IL-12 mRNA levels were compared to those before or after cross-linking by using paired, two-tailed Student *t* tests. A P value of <0.05 was considered significant.

RESULTS

CD1d downregulation in HPV-related lesions and cancer cell lines. Since CD1d expression in human mucosa and skin has been demonstrated by immunohistochemistry using the anti-CD1d NOR3.2 MAb (2, 9, 12, 26), we examined immunostaining of human normal ectocervix or HPV-related lesions with NOR3.2 (Fig. 1). Immunostaining for CD1d was performed on formalin-fixed, paraffin-embedded tissue sections of normal or inflamed ectocervical epithelium, cervical intraepithelial neoplasia 1 (CIN1), cervical cancer, and cervical condyloma (obtained under IRB approval through the University of Tokyo, Faculty of Medicine). To examine alterations in CD1d expression in the presence of high-risk HPV and low-risk HPV subtypes, HPV16-positive CIN1 or cancer lesions and HPV6-positive condyloma acuminata specimens were compared to each other and to HPV-negative normal and inflamed ectocervical epithelial controls. Immunoreactivity with the NOR3.2 MAb was noted in the basal and parabasal epithelial cells of normal and inflamed ectocervical epithelia that are known to express early HPV genes (E5, E6, and E7; Fig. 1) (44). In inflamed epithelium, the immunoreactivity appeared to be intensified compared to normal epithelium. CD1d expression is known to be enhanced by inflammatory cytokines (10). NOR3.2 immunoreactivity is essentially absent in HPV16-positive CIN1, HPV16-positive cancer, and HPV6-positive condyloma lesions (Fig. 1). To statistically analyze alterations in CD1d expression, a total of 45 clinical specimens from normal controls and HPV-related lesions were immunostained with NOR3.2 (Table 1). NOR3.2 immunoreactivity was

TABLE 1. Immunoreactivity with NOR3.2 anti-CD1d MAb in cervical epithelium of various lesions

Histological status	HPV status[a]	CD1d (no. of cases)		% Positive[b]
		Positive	Negative	
Normal/inflamed		9	1	90.0
CIN1 and CIN2	HR-HPV(+)	0	7	0
CIN3	HR-HPV(+)	2	16	11.1
Cancer	HR-HPV(+)	0	7	0
Condyloma	HPV6(+)	0	3	0

[a] HR-HPV(+), any high-risk HPV positive.
[b] $P = 0.0001$ (exact Cochran-Armitage Trend test).

mostly limited to the HPV-negative normal or inflamed ectocervical epithelial samples similar to those represented in the first two panels of Fig. 1. NOR3.2 immunoreactivity was absent in all CIN1 and CIN2, cervical cancer, and condyloma lesions. Among CIN3 samples, two lesions showed NOR3.2 immunoreactivity, whereas 16 lesions did not. Using trend analysis, we were able to demonstrate an association between decreased CD1d immunoreactivity and progression of cervical neoplastic lesions with statistical significance ($P = 0.0001$).

Although HPV E5 is not expressed in cervical cancer cells (16), immunohistochemical data demonstrated that CD1d expression was also abrogated in cervical cancer lesions. To address the mechanisms underlying CD1d downregulation in cervical cancers, we examined the level of CD1d transcription and CD1d expression at the cell surface in several cervical cancer cell lines (Fig. 2). As a positive control, we created cell transfectants that stably expressed CD1d. To avoid the potential influence of endogenous HPV protein expression, an HPV-negative cervical cancer cell line, C33A, was used for our CD1d transfectants. We used a retrovirus vector to transduce the CD1d gene into these cells and established the stable cell line, C33A/CD1d via neomycin selection. Flow cytometry revealed strong expression of CD1d on the cell surface of C33A/CD1d cells. Cd1d was not expressed on the cell surface of C33A control cells or in other cancer cell lines (Fig. 2A). To examine the level of CD1d transcription in these same cells, cDNA was produced via RT of total RNA from each cell line and subjected to PCR using primer pairs specific for CD1d. The expected single band representing CD1d was observed on agarose gels only in C33A/CD1d cells (Fig. 2B). These data indicated that CD1d expression was abrogated prior to or during transcription the tested cervical cancer cell lines.

Cell surface expression of CD1d decreases in HPV E5-expressing epithelial cells. HPV E5 has been reported to inhibit cell surface expression of HLA class I molecules by interfering with their trafficking to the cell surface (1, 2, 3, 21, 30). Since CD1d and HLA class I heavy chains utilize an identical intracellular pathway to traffic from the ER to the cell surface, we hypothesized that HPV E5 may also interfere with surface CD1d expression at a posttranscriptional level. To verify our immunohistochemical data and study CD1d trafficking in the presence of E5 *in vitro*, we created HPV6 and HPV16 E5 stably transfected cell lines using C33A/CD1d cells. Since the E5 protein is less than 10 kDa in size, the production of an anti-E5 antibody would be difficult. Instead, E5 proteins were tagged with FLAG and detected by Western blotting or immunostaining with an anti-FLAG antibody. FLAG-tagged HPV6 or HPV16 E5 genes were transduced into the C33A/CD1d cells by using retrovirus vectors. To control for the influence of retrovirus infection and the presence of the expression vector, C33A/CD1d cells were infected with empty retrovirus vectors. Retrovirus-infected cells were exposed to puromycin, and E5-expressing C33A/CD1d cells were established (C33A/CD1d-6E5, -16E5, and -empty). In Fig. 3A, lanes 5 and 6, show PCR products derived from cDNA generated by RT of total RNA from C33A/CD1d-6E5 and -16E5 cells. Lanes 2 and 3 in the same figure show PCR products derived from corresponding expression plasmid DNA. FLAG-6E5 and -16E5 were transcribed in C33A/CD1d-6E5 and -16E5 cells, respectively. Using Western immunoblotting and an anti-FLAG MAb, FLAG-6E5 and -16E5 proteins were detected as immunoreactive bands at an approximate size of 10 kDa in lanes 1 and 2, respectively (Fig. 3B).

We next examined the expression of CD1d at both mRNA and protein levels in the presence or absence of HPV E5. CD1d transcription levels in C33A/CD1d cells were unaffected by the presence of E5 or of empty vector compared to naive

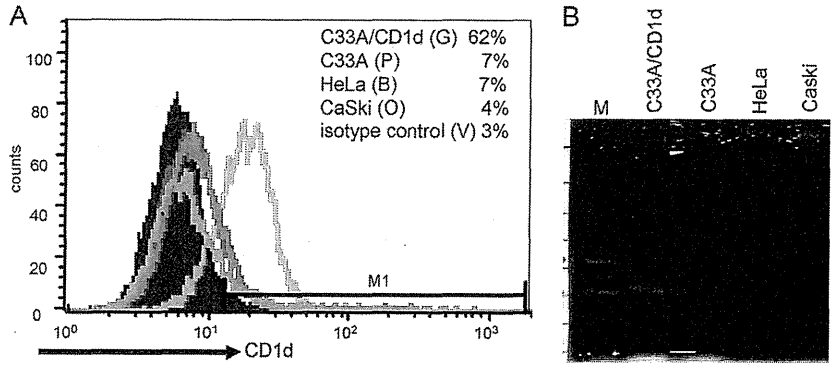

FIG. 2. CD1d alterations in cancer cell lines. (A) Cell surface expression of CD1d in C33A (pink line), HeLa (blue line), CaSki (orange line), and C33A/CD1d (green line) cells. All cells were stained with an anti-CD1d primary MAb (NOR3.2; 1:100 dilution) and a PE-conjugated goat anti-mouse immunoglobulin secondary antibody (1:20 dilution). Background staining of the cells using an isotype-matched control antibody is also shown (filled region). Cells were suspended in 1% paraformaldehyde and analyzed by using a FACSCalibur flow cytometry system. (B) Transcription of CD1d. cDNA was produced via RT of 1 μg of total RNA from each cell line and amplified by PCR with primer pairs specific for CD1d. PCR products were separated over an agarose gel containing ethidium bromide.

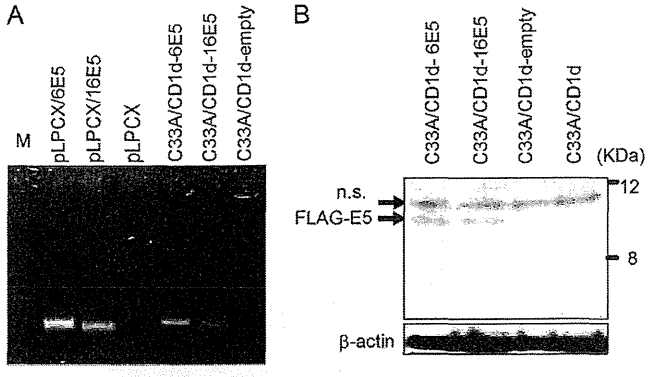

FIG. 3. HPV E5 detection in HPV E5-transformed C33A/CD1d cells. (A) Transcription of HPV E5. cDNA was produced via RT of 1 μg of total RNA from each cell line and amplified by PCR with primer pairs specific for HPV16 E5 and HPV6 E5. PCR products were separated over an agarose gel containing ethidium bromide. Lanes 5 and 6 display PCR products derived from C33A/CD1d-6E5 and -16E5 cDNA, respectively, while lanes 2 and 3 show PCR products derived from corresponding expression plasmid DNA. Lanes 4 and 7 represent negative control plasmid and cell lines lacking E5, respectively. (B) Translation of HPV E5. Fifty-microgram aliquots of protein lysates from each cell line were analyzed by Western immunoblotting with antibodies against the FLAG tag (1:500 dilution) and β-actin (loading control).

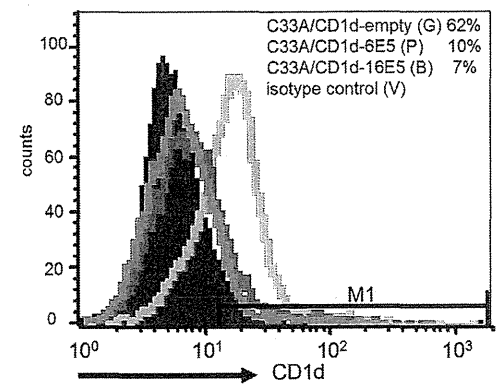

FIG. 5. Cell surface expression of CD1d in C33A/CD1d-empty (green line), C33A/CD1d-6E5 (pink line), and -16E5 (blue line) cells. All cells were stained with an anti-CD1d primary MAb (NOR3.2; 1:100 dilution) and a PE-conjugated goat anti-mouse immunoglobulin secondary antibody (1:20 dilution). Background staining of the cells with an isotype-matched control antibody is also shown (filled region). Cells were suspended in 1% paraformaldehyde and analyzed using a FACSCalibur flow cytometry system.

C33A/CD1d cells (Fig. 4A). In contrast, the 48-kDa, mature glycosylated form of the CD1d heavy chain (HC) that was detected in naive C33A/CD1d and C33A/CD1d-empty cells was completely abrogated in C33A/CD1d-6E5 and barely detectable in the C33A/CD1d-16E5 cells (Fig. 4B, lanes 1, 4, 2, and 3, respectively). The presence of HPV6 and HPV16 E5 drastically inhibited the maturation of CD1d HCs. Flow cytometry was used to analyze the effect of HPV E5 on cell surface expression of CD1d in the C33A/CD1d cells harboring E5-expressing or empty vector (Fig. 5). CD1d was expressed by

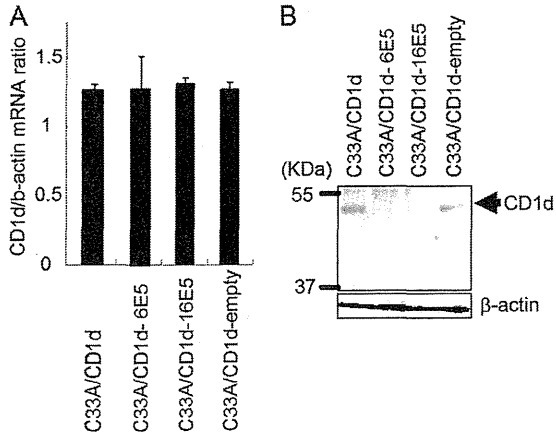

FIG. 4. CD1d heavy-chain transcription and translation in C33A/CD1d, C33A/CD1d-empty, C33A/CD1d-6E5, and C33A/CD1d-16E5 cells. (A) Transcription of CD1d HC. The mRNA levels of CD1d were analyzed by quantitative RT-PCR using SYBR green methodology. CD1d mRNA levels were normalized to β-actin. (B) Fifty-microgram aliquots of protein lysates from each cell line were analyzed by Western immunoblotting with a peroxidase-labeled anti-CD1d NOR3.2 MAb (1:200 dilution) and a β-actin loading control.

the majority of C33A/CD1d-empty cells but absent in >70% of C33A/CD1d-6E5 or -16E5 cells (Fig. 5).

To confirm the effect of E5 on endogenous CD1d, we used a vaginal epithelial cell line immortalized via HPV16 E6/E7 transduction of primary cells collected from normal human vaginal epithelium and subsequently well characterized as possessing histological and immunological characteristics identical to those of primary epithelial cells (18). We have previously reported the endogenous expression of functional CD1d molecules on the surface of these cells (25). Since vaginal epithelial cells are well-known targets of genital HPV, these cells were considered to be useful as an *in vitro* model for *in vivo* HPV infections. FLAG-tagged HPV6 or HPV16 E5 genes were transduced into these vaginal cells by using retrovirus vectors (Vag-6E5 and -16E5). We then examined the expression of CD1d at various levels in the presence or absence of HPV E5 (Fig. 6). RT-PCR and Western blotting revealed that CD1d transcription was unaffected by the presence of E5, but the 48-kDa CD1d HC product clearly decreased in Vag-6E5 and -16E5 cells compared to naive and Vag-empty cells (Fig. 6A). Flow cytometry confirmed the decreased cell surface expression of CD1d in 6E5-expressing vaginal epithelial cells (Fig. 6B).

E5-expressing epithelial cells retain CD1d in the ER. To demonstrate the intracellular localization of CD1d heavy chains in C33A/CD1d cells harboring HPV-6E5 and -16E5, immunofluorescence confocal microscopy was performed with an anti-CD1d MAb (NOR3.2) combined with either an anti-FLAG MAb that detects FLAG-E5 proteins, an ER-specific marker (ER tracker) or DAPI (Fig. 7). In C33A/CD1d-empty control cells, dual labeling for CD1d and the nucleus (DAPI) verified that CD1d could be detected in a diffuse pattern throughout the intracellular space, with increased accumulation near the cell surface but not in the perinuclear area (Fig. 7, upper image). In contrast, decreased amounts of CD1d could be detected in C33A/CD1d-6E5 and -16E5 cells and CD1d proteins were localized to perinuclear areas near the ER. CD1d and ER signals merged in perinuclear areas (pink

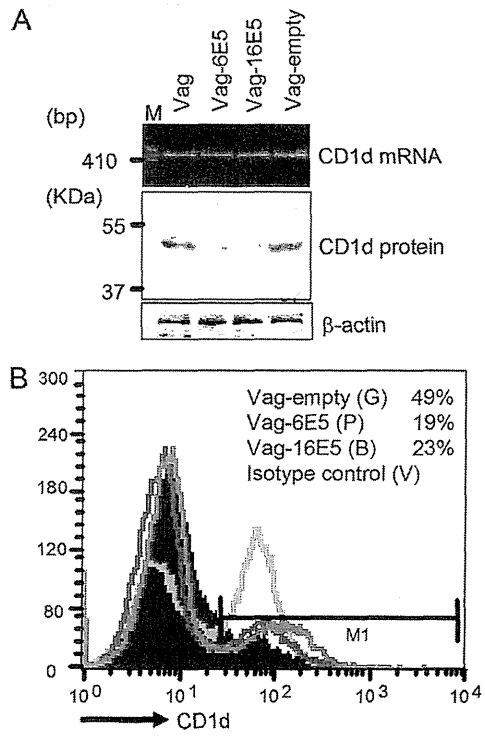

FIG. 6. CD1d downregulation in alternate genital keratinocytes in the presence of 6E5 and 16E5. (A) HPV6 and HPV16 E5 genes were transduced into vaginal epithelial cells established from normal human vaginal epithelium (17) and named Vag-6E5 and Vag-16E5, respectively. PCR products derived from cDNA generated by reverse transcription using 1 μg of total RNA from each of the vaginal cell lines were separated over an ethidium bromide-containing agarose gel. Fifty-microgram aliquots of protein lysates from each vaginal cell line were analyzed by Western immunoblotting with a peroxidase labeled anti-CD1d NOR3.2 MAb (1:200 dilution) and a β-actin loading control. (B) Vag-empty (green line), Vag-6E5 (pink line), and Vag-16E5 (blue line) were stained with an anti-CD1d primary MAb (NOR3.2; 1:100 dilution) and a PE-conjugated goat anti-mouse immunoglobulin secondary antibody (1:20 dilution). Background staining of the cells using an isotype-matched control antibody is also shown (filled region). Cells were suspended in 1% paraformaldehyde and analyzed by using a FACSCalibur flow cytometry system.

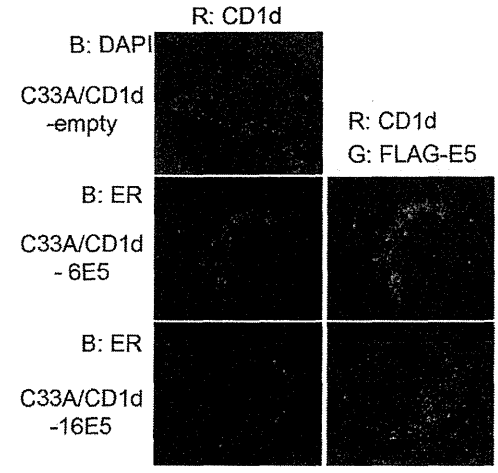

FIG. 7. CD1d trafficking in the presence or absence of E5. C33A/CD1d-empty, C33A/CD1d-6E5, or C33A/CD1d-16E5 cells were seeded onto coverslips. All of the cells were immunostained with an anti-CD1d MAb (NOR3.2, red). C33A/CD1d-empty were also exposed to DAPI (blue), and C33A/CD1d-6E5 or -16E5 cells were exposed to ER tracker (blue) and an anti-FLAG MAb (green). Cells were then visualized by using fluorescence confocal microscopy. Orange to yellow signals represent colocalization of CD1d and E5 within the ER.

signals), suggesting that the majority of CD1d is within the ER (Fig. 7, images on the left). Dual labeling for CD1d and FLAG-E5 verified the colocalization of CD1d and E5 within the ER (orange to yellow signals), while nonmerged FLAG-E5 signals were present in the perinuclear area (pure green), suggesting the presence of E5 in the GA in the absence of CD1d (Fig. 7, images on the right). The results of immunofluorescence microscopy support our biochemical and flow cytometry data showing that mature CD1d protein levels decrease and CD1d fails to traffic to the cell surface in HPV E5-expressing cells.

HPV E5 interacts with calnexin in the ER. Previous biochemical studies have reported that HPV16 E5 interacts with calnexin and that these interactions interfere with the modification of HLA class I heavy chains that typically occurs in the ER (21). The role of calnexin and/or calreticulin in the formation of the second disulfide bond of CD1d HCs in the ER is well described (24). We therefore hypothesized that E5 interacts with calnexin in the ER and may impair calnexin-mediated CD1d folding. This, in turn, could interrupt appropriate trafficking of CD1d to the surface of HPV-infected cells. To address the hypothesis, we examined the interaction of E5 with calnexin using immunoprecipitation. Total cell lysates obtained from C33A/CD1d-empty, -6E5, and -16 E5 cells were incubated with anti-FLAG MAb conjugated beads. FLAG-E5-bound proteins were immunoprecipitated and analyzed by immunoblotting with an anti-calnexin MAb. A band with an apparent molecular mass of 90 kDa and corresponding to calnexin was detected in C33A/CD1d-6E5 and -16 E5 cells, but not C33A/CD1d-empty cells, biochemically demonstrating interaction between E5 with calnexin (Fig. 8A).

To visually demonstrate the colocalization of CD1d and calnexin, C33A/CD1d-empty, -6E5, and -16E5 cells were dually stained with anti-CD1d NOR3.2 and anti-calnexin MAbs and examined by using confocal microscopy. Again, NOR3.2-reactive CD1d was detected throughout the intracellular space in C33A/CD1d-empty cells. In contrast, the majority of CD1d molecules in C33A/CD1d-6E5 or -16E5 cells localized to the perinuclear area (Fig. 8B, images on left). Calnexin detection was rendered as green signals. These mostly localized to perinuclear areas in E5-expressing cells and correspond to the location of ER (Fig. 8B, center images). Although some merge images (yellow signals) could be detected in each cell line, the merge patterns differed between C33A/CD1d-empty and E5-expressing cells (Fig. 8B, images on the right). In C33A/CD1d-empty cells, the calnexin and CD1d signals were mostly distinct and but those that did colocalize appeared to follow the synthetic pathway for type I proteins. In contrast, CD1d in the E5-expressing cells completely colocalized with calnexin, confirming our biochemical data demonstrating physiologic interaction between calnexin and CD1d in the C33A/CD1d-6E5 and -16E5 cells.